Computational and Structural Biotechnology Journal 23 (2024) 3634–3650

Contents lists available at ScienceDirect

Computational and Structural Biotechnology Journal

journal homepage: www.elsevier.com/locate/csbj

Research Article

The complement C3a/C3aR pathway is associated with treatment resistance to gemcitabine-based neoadjuvant therapy in pancreatic cancer

Saimeng Shi [a,b,c,d,1], Longyun Ye [a,b,c,d,1], Kaizhou Jin [a,b,c,d,1], Xianjun Yu [a,b,c,d,*], Duancheng Guo [a,b,c,d,*], Weiding Wu [a,b,c,d,*]

[a] Department of Pancreatic Surgery, Fudan University Shanghai Cancer Center, Shanghai 200032, China
[b] Department of Oncology, Shanghai Medical College, Fudan University, Shanghai 200032, China
[c] Shanghai Pancreatic Cancer Institute, Shanghai 200032, China
[d] Pancreatic Cancer Institute, Fudan University, Shanghai 200032, China

ARTICLE INFO

Keywords:
Pancreatic cancer
Gemcitabine resistance
Complement C3a
C3aR antagonist
Neoadjuvant therapy

ABSTRACT

Gemcitabine is a standard first-line drug for pancreatic cancer chemotherapy. Nevertheless, gemcitabine resistance is common and significantly limits its therapeutic efficacy, impeding advancements in pancreatic cancer treatment. In this study, through a comprehensive analysis of gemcitabine-resistant cell lines and patient samples, 39 gemcitabine resistance-associated risk genes were identified, and two distinct gemcitabine response-related phenotypes were delineated. Through a combination of bioinformatics analysis and in vivo and in vitro experiments, we identified the C3a/C3aR signaling pathway as a pivotal player in the development of gemcitabine resistance in pancreatic cancer. We found that activation of the C3a/C3aR signaling pathway promoted the proliferation, migration and gemcitabine resistance of pancreatic cancer cells, while the C3aR antagonist SB290157 effectively counteracted these effects by impeding the activation of the C3a/C3aR pathway. Our study reveals the fundamental role of complement C3a in the progression of pancreatic cancer, suggesting that complement C3a may serve as a promising biomarker in pancreatic cancer.

1. Introduction

Pancreatic cancer is a complex and highly lethal malignant tumor of the digestive system, and its incidence and mortality are increasing annually worldwide [1,2]. Currently, pancreatic cancer ranks as the seventh leading cause of cancer-related death worldwide and is expected to become the second leading cause of cancer-related death in Western countries in the foreseeable future [3]. Surgical intervention remains the sole method for the radical treatment of pancreatic cancer. Regrettably, approximately 80–85 % of patients miss the opportunity for surgical resection due to diagnosis in the advanced stage, which is a consequence of the rapid progression and early metastasis of pancreatic cancer [4]. Therefore, pancreatic cancer is recognized as the “king of cancer”.

In recent years, advancements in adjuvant chemotherapy drugs and pre- and postoperative chemotherapy regimens for pancreatic cancer have contributed to notable improvements in patient survival rates. Gemcitabine is the standard first-line drug for the treatment of advanced or metastatic pancreatic cancer, but the widespread emergence of drug resistance has undermined its therapeutic effectiveness, resulting in an overall response rate of only approximately 20 % [5,6]. The main reason is that cancer cells can escape the cytotoxic effects of gemcitabine through a variety of internal and external cellular mechanisms [7,8]. For example, in the tumor microenvironment (TME) of pancreatic cancer, the dense desmoplastic stroma constitutes a physical barrier to gemcitabine delivery; the accumulation of multiple immune suppressor cells promotes the formation and development of an immunosuppressive microenvironment; and abundant inflammatory factors also play important roles. Previous studies have shown that C-X-C motif chemokine ligand 13 (CXCL13) acts on its receptor C-X-C motif chemokine receptor 5 (CXCR5), inducing the chemotaxis of $CD8^+$ T cells and B cells to the pancreatic cancer microenvironment [9,10]; CCL25 promotes the recruitment of T cells [11,12]; CCL21 and its receptor CCR7 are involved

* Corresponding authors at: Department of Pancreatic Surgery, Fudan University Shanghai Cancer Center, Shanghai 200032, China.
E-mail addresses: yuxianjun@fudanpci.org (X. Yu), guoduancheng@shca.org.cn (D. Guo), wuweiding@fudanpci.org (W. Wu).
[1] These authors contributed equally to this work.

https://doi.org/10.1016/j.csbj.2024.09.032
Received 30 June 2024; Received in revised form 21 September 2024; Accepted 27 September 2024
Available online 5 October 2024

in the aggregation and infiltration of cytotoxic tumor-infiltrating lymphocytes in the TME [13,14]; and a variety of interleukins (such as IL-12, IL-20, IL-23 and IL-18) and their receptors participate in the inflammatory response and promote antitumor immunity [15–17]. Changes in the tumor immune microenvironment and the levels of inflammatory factors may strongly affect the efficacy of chemotherapy. In addition, cancer cells can modify themselves via DNA damage repair, epithelial–mesenchymal transition (EMT) and other ways to escape the killing effects of cytotoxic drugs. Therefore, in-depth exploration of the mechanisms underlying gemcitabine chemotherapy resistance in pancreatic cancer is crucial and could aid in the development of more effective treatment strategies to combat gemcitabine resistance. Moreover, the systemic administration of gemcitabine is associated with considerable side effects. Consequently, an important avenue for research is the pursuit of targeted therapeutic drugs with high efficacy and low toxicity.

In the current study, we identified a set of 39 risk genes associated with gemcitabine resistance via RNA sequencing analysis of gemcitabine-resistant pancreatic cancer cell lines and clinical patient samples [18]. With a total of 754 patient samples from 6 public databases, consensus cluster analysis was performed to identify different clusters according to the expression profiles of these 39 risk genes [19]. According to their distinct half-maximal inhibitory concentration (IC50) values, these two clusters were defined as gemcitabine-resistant (GR) group and gemcitabine-sensitive (GS) group. There were significant differences in the inflammatory response and immune cell infiltration between these two groups. Moreover, a machine learning-derived prognostic profile (MLDPP) based on the 39 risk genes was established via a comprehensive approach based on machine learning. Patients with high MLDPP had poorer survival rates and were less sensitive to gemcitabine treatment.

Finally, by integrating gemcitabine response-related, immune infiltration-related and gemcitabine IC50-related differentially expressed genes, the complement C3a receptor (gene *C3aR1*) was identified as the only common differentially expressed gene. Complement C3a and its receptor C3aR are abnormally highly expressed in pancreatic cancer and are significantly associated with poor survival and a poor response to gemcitabine neoadjuvant therapy. Subsequent in vitro experiments revealed that C3a activated pancreatic cancer cells, promoting their proliferation and migration ability while reducing their gemcitabine sensitivity. Conversely, pharmacological inhibition of the C3a/C3aR signaling pathway reversed these changes and inhibited the progression of pancreatic cancer. In conclusion, our study reveals 39 risk genes that are closely associated with gemcitabine resistance in pancreatic cancer and highlights the important role of the C3a/C3aR signaling pathway in promoting malignant phenotypes. From the perspective of complement system activation, our research comprehensively demonstrated that complement C3a may act as a bypass pathway to increase gemcitabine resistance in pancreatic cancer. Moreover, we confirmed the therapeutic potential of the C3aR1 inhibitor SB290157 in a mouse model of pancreatic cancer; notably, no significant toxic side effects were observed, suggesting that SB290157 is a promising targeted clinical treatment strategy.

2. Materials and methods

2.1. Data acquisition

Online RNA sequencing data was download from TCGA, GEO and ArrayExpress by using R packages “TCGAbiolinks”, “GEOquery” and “ArrayExpress”. Online datasets included TCGA-PAAD, GSE21501, GSE57495, GSE79668, GSE85916, and E-MTAB-6134.

2.2. Identification of gemcitabine resistance associated risk genes, gemcitabine resistant (GR)-phenotype and gemcitabine sensitive (GS)-phenotype

Differentially expressed genes between GR subline and the parental line were obtained from the RNA sequencing results of Chen Lab [18]. 3 pairs of pancreatic cancer tissue samples were obtained from gemcitabine neoadjuvant resistant/sensitive patients from Fudan University Shanghai Cancer Center (FUSCC). All six patients were pathologically and clinically diagnosed as pancreatic ductal adenocarcinoma. At least 3 cycles of chemotherapy prior to surgery were applied to these patients, with the chemotherapy regimen as gemcitabine combined with albumin-paclitaxel. The efficacy of chemotherapy was comprehensively evaluated according to the changes of radiological metrics and serum carbohydrate antigen (CA)19–9 [20]. Detailed clinical characteristics of these six patients can be obtained in Fig. S1. RNA sequencing and subsequent analysis were performed to identify the differentially expressed genes. Gemcitabine resistance associated risk genes were obtained by intersecting differentially expressed genes from cell lines and patients. Based on these risk genes, a consensus clustering algorithm was performed to identify GR-phenotype and GS-phenotype.

2.3. Evaluation of the tumor immune and inflammatory microenvironment in pancreatic cancer

In previous studies, about 122 inflammatory modulators, including chemokines, interferons, cytokines, and their receptors have been identified [21]. TIP (Tracking Tumor Immunophenotype) is a meta-server that conceptualizes the anti-cancer immune response as a series of stepwise events of the cancer-immune cycle, which include: (1) the release of cancer cell antigens; (2) the presentation of cancer antigens; (3) the initiation and activation; (4) the migration of immune cells to the tumor; (5) the infiltration of immune cells in the tumor microenvironment; (6) the recognition of cancer cells by T cells; (7) the killing of cancer cells [22]. Related genes were extracted from the TIP server, and the infiltration of various immune cells (such as T cells, B cells, DC cells, NK cells and macrophages) was evaluated by seven immune algorithms (including CIBERSORT [23], ssGSEA [24], XCELL [25,26], TIMER [27,28], Quantiseq [29,30], MCPcounter [31] and EPIC [32]). The ESTIMATE algorithm was also used to score immune cell infiltration and the tumor microenvironment. Typical tumorigenesis-related gene sets (such as EMT, DNA damage repair, etc.) were annotated based on the previous studies [33].

2.4. Construction of MLDPP by integrative machine learning algorithms

Based on 39 gemcitabine-resistance associated risk genes, univariate Cox regression analysis was used to identify features between the two clusters. Based on the 10-fold cross-validation approaches, 10 machine learning algorithms are randomly combined to generate 101 combined algorithms. These 101 combination algorithms are constructed in TCGA-PAAD, GSE21501, GSE57495, GSE79668, GSE85916, E-MTAB-6134 and joint cohorts and the optimal signature was valued by calculating its average C-index across all cohorts.

2.5. Correlation with drug sensitivity

Public pharmacogenomics databases Cancer Genome Project (CGP, ftp://ftp.sanger.ac.uk/pub4/cancerrxgene/releases) was used to analyze the correlation between the expression of gemcitabine resistance-associated risk genes and the chemotherapeutic drugs sensitivity. Cancer Therapeutics Response Portal (CTRP, https://portals.broadinstitute.org/) was used to predict chemotherapy drugs sensitivity. The R packages “PRRophetic” and “oncopredict” were used for prediction.

2.6. Patients and specimens

The clinical tissue samples used in this study were collected from pancreatic cancer patients who underwent radical surgery at FUSCC from October 2011 to June 2014. Clinical tissue samples of neoadjuvant chemotherapy were collected from patients with pancreatic cancer who underwent preoperative neoadjuvant chemotherapy at FUSCC between October 2015 and August 2019. The chemotherapy regimen used was gemcitabine combined with albumin—paclitaxel. The Response Evaluation Criteria in Solid Tumors (RECIST, Version 1.1) were used to classify the radiological tumor response to chemotherapy into four grades: complete response (CR), partial response (PR), progressive disease (PD), and stable disease (SD) [34,35]. The efficacy of chemotherapy was comprehensively evaluated according to changes in radiological metrics and serum CA19–9. According to RECIST 1.1 and serum CA19–9 changes, we categorized patients who underwent neoadjuvant chemotherapy into a GS group (including those with a response evaluation of CR or PR and decreased serum CA19–9 level) and a GR group (including those with a response evaluation of PD or SD without a decrease in the serum CA19–9 level) [20,36,37].

2.7. Cell culture, transfection and the construction of stable cell line

Human pancreatic cancer cell lines Panc-1 and mouse pancreatic cancer cell lines Panc-02 were purchased from Chinese Academy of Sciences. Cells were cultured in high glucose DMEM with 10 % fetal bovine serum and 1 % penicillin-streptomycin and kept at 37 ℃, 5 % carbon dioxide in a humidified incubator. All cell lines have been authenticated using STR DNA finger-printing and tested with no mycoplasma contamination.

Lentiviral plasmids were purchased from Tsingke Biotechnology. HEK293T cells were seeded in 100 mm dishes to a density of 60 % to 70 %. Lipofectamine™ 3000 (L3000075, Thermo Fisher,) was used as a gene delivery carrier. Panc-1/Pan-02 cells were infected with the lentiviral particle-enriched supernatant, and stable cell lines were constructed with 10 μg/ml puromycin. The shRNA sequences are as follow:

sh-Scr: CCTAAGGTTAAGTCGCCCTCG;.
shC3aR#1 (human): GCTGATGTGGTCTCACCTAAA;.
shC3aR#2 (human): TCACTACAGACAACCATAATA;.
shC3aR#1 (mouse): CCAGAAAGCAATTCTACTGAT;.
shC3aR#2 (mouse): CCCATCCATCATTATTCTCAA.

2.8. Animal model and drug treatment experiment

LSL-Kras$^{G12D/+}$*LSL-Trp53*$^{R172H/+}$*Pdx-1-Cre* (KPC) transgenic mice were generated by Dr. Wu as described previously [20]. Female BALB/c-nu mice, aged 4–6 weeks, were purchased through the Laboratory Animal Center of FUSCC for the construction of subcutaneous tumor models. About 5×10^6 Panc-1 cells were injected subcutaneously in 100 μL PBS, and the tumor volume was calculated as (width^2 ×length)/2. In in vivo experiments with C3aR knockdown, 10 female BALB/c-nu mice, aged 5 weeks, were randomly divided into 2 groups and respectively injected with control Panc-1 (/Panc-02) cells and C3aR-deficient Panc-1 (/Panc-02) cells to construct subcutaneous tumor model. Tumor volume was measured and calculated every 3 or 2 days. When the tumor diameter reached 15 mm, tumor samples were collected and photographed. In in vivo experiment with the treatment of C3aR antagonist SB290157, the mice were randomly grouped when the tumor volume reached about 200 mm^3 to receive treatment. 3 % DMSO in MCT (0.5 % methyl cellulose containing 0.2 % Tween-80, Solarbio) was used as vehicle where the C3aR antagonists SB290157 and gemcitabine were dissolved. Each group was respectively treated with vehicle, SB290157 (20 mg/kg), gemcitabine (20 mg/kg), or SB290157(20 mg/kg) combined with gemcitabine (20 mg/kg) once a day for two weeks. When the subcutaneous tumor was constructed with Panc-02 cells, murine SB290157 was used accordingly. At the end of the treatment, tumors were collected for sections, RNA and protein samples.

2.9. Immunohistochemistry (IHC) and immunofluorescent staining (IF)

Formalin-fixed and paraffin-embedded tissue samples were sent to Wuhan Servicebio Technology for IHC and IF staining. IHC/IF staining, expression evaluation and the cohort grouping were performed as described previously [20]. IHC staining with antibodies against C3 (1:2000, ab200999, Abcam), human C3a (1:100, ab36385, Abcam), mouse C3a (1:100, X-Y Biotechnology) and C3aR1 (1:50, K006964P, Solarbio) were applied to detect protein expression. Concrete methods of IHC scoring have been described in our previous studies [20]. IF staining with antibodies against Ki-67(1:200, 27309–1-AP, Proteintech), anti-Cleaved-caspase 3 (CC3, 1:1000, 9664S, Cell Signaling Technology, CST).

2.10. Enzyme-linked immunosorbent assay (ELISA)

ELISA was used to quantified C3a levels in the tumor tissues. ELISA kits were purchased from Shanghai YEPCOME Biotechnology Co., Ltd, and detected according to the manufacturer's instructions.

2.11. 5-Ethynyl-2′-deoxyuridine (EdU) assay

BeyoClick™ EdU-594 kit (Beyotime) was applied for EdU assay. Cells were plated in 24-well plates in triplicate. After 48 h, 10 μM EdU was added and incubated for 2 h at 37 ℃. Then cells were fixed with 4 % paraformaldehyde, and then permeated with 2 %Triton X-100. Click Addictive Solution was used to develop color. Finally, a fluorescence microscope was used to obtain images.

2.12. Transwell assay

1×10^4 Panc-1/Panc-02 cells were suspended in 200 μL serum-free medium in the Matrigel-free upper chamber (24-well, 8 μm pore diameter, CLS3422, Corning), and the lower chamber was added with 400 μL full medium. After culturing for 12 h, lower chamber cells were fixed and stained with Crystal Violet. The number of migrated cells in a random area was counted, with 5 fields per chamber were calculated.

2.13. CCK-8 assay

Cell Counting Kit-8 (CCK-8, B34302, Selleck) was used to quantify cell viability. Cells were plated in 96-well plates in triplicate, and treated with the corresponding reagents for 48 h. Then CCK-8 reagent was added to each well and incubated at 37 ℃ for 2 h. Optical density at 450 nm was measured with a microplate reader.

2.14. Western blotting

Total protein of tissue samples or cell lines were extracted from RIPA lysis buffer, and then separated by SDS-PAGE gels and transferred to PVDF membranes. PVDF membrane was incubated with the primary antibody at 4 ℃ overnight, and with secondary antibody at room temperature for 2 h. The protein bands were displayed on the Clinx chemiluminescence apparatus using the chromogenic solution. Using Clinx Chemiluminescence Instrument to visualize the protein bands. Antibodies used for Western blotting are as follows: anti-GAPDH (1:50000; 60004–1-Ig, Proteintech); anti-C3aR1 (1:500; A6361, ABclonal); anti-C3aR1 (1:2000; A24665, ABclonal); goat anti-rabbit IgG secondary antibody HRP conjugated (1:5000; L3012, Signalway Antibody, Greenbelt, MD, USA); goat anti-mouse IgG secondary antibody HRP conjugated (1:5000; L3032, Signalway Antibody).

2.15. Conventional PCR and real-time quantitative PCR (qPCR)

RNAeasy™ Animal RNA Isolation Kit with Spin Column (R0027, Beyotime) was used to extract total RNA from cell samples. HiScript III 1st Strand cDNA Synthesis Kit (+gDNA wiper) (R312, Vazyme) was used to synthesize cDNA. NanoDrop One spectrophotometer was used to detect the RNA quality and concentration. Conventional PCR was performed following the standard protocols. Real-time qPCRs were performed using Taq Pro Universal SYBR qPCR Master Mix (Q712, Vazyme) and ABI 7500 TaqMan Real-Time PCR Detection System. $2^{-\Delta\Delta Ct}$ method was used to calculate. qPCR primer sequences are as follows:

GAPDH (human):
forward: 5′-GTCTCCTCTGACTTCAACAGCG-3′;.
reverse: 5′-ACCACCCTGTTGCTGTAGCCAA-3′;.
GAPDH (mouse):
forward: 5′-CATCACTGCCACCCAGAAGACTG-3′;.
reverse: 5′-ATGCCAGTGAGCTTCCCGTTCAG′;.
C3AR1 (human):
forward: 5′-CCTGCTGATGTGGTCTCACCTA-3′;.
reverse: 5′-CCTTGTGGTAGCTCAGACTCGT-3′;.
C3AR1 (mouse):
forward: 5′-CTGGCGTAAAGATGAAGACGACC-3′;.
reverse: 5′-CCAGTGTCCTTGGAGAATCAGG-3′;.

2.16. Chemical and protein reagents

Recombinant human complement C3a protein (MedChemExpress, MCE; HY-P7862), recombinant mouse complement C3a protein (MCE; HY-P7863) and C3aR antagonist, SB290157 (TargetMol) were used according to the manufacturer's instructions. C3a was used for pancreatic cancer cell stimulation at the indicated concentrations. SB290157 was used at 200 nM for cell treatment and 20 mg/kg for in vivo experiments.

2.17. RNA sequencing

TRIzol reagent (15596018, Thermo Fisher Scientific) was used to extract RNA from tissue samples. And RNA sequencing was performed by Novogene Co., Ltd (Beijing, China). Using R-4.1.3 software to analyze the sequencing results.

2.18. Statistical analysis

All experiments were repeated at least triplicate. Data were analyzed using GraphPad Prism 9 software and presented as the mean ± SD. Student's t-test was used to compare continuous variables between two groups. Chi-square or Fisher exact test were used to compare categorical variables. Kaplan-Meier survival curves and Log-rank test were used to analyze survival data. $P < 0.05$ was considered statistically significant.

3. Results

3.1. Identification of gemcitabine response-related phenotypes via unsupervised clustering

We collected pancreatic cancer tissues from 6 patients, 3 of whom were sensitive to neoadjuvant therapy with gemcitabine (GS) and 3 of whom were not (GR). All six patients were pathologically and clinically diagnosed with pancreatic ductal adenocarcinoma. At least 3 cycles of chemotherapy prior to surgery were applied to these patients, and the chemotherapy regimen used was gemcitabine combined with albumin—paclitaxel. The efficacy of chemotherapy was comprehensively evaluated according to changes in radiological metrics and serum CA19–9 [20]. The detailed clinical characteristics of these six patients are described in Fig. S1. By RNA sequencing, we identified and analyzed the differentially expressed genes between pancreatic cancer tissues from GS and GR patients (Table S1). In a previous study, Shi Chen et al. constructed a GR subline of the pancreatic cancer cell line Panc-1 through repeated gemcitabine induction and identified the differentially expressed genes between the parental line and the GR subline via RNA sequencing [18]. Through a comprehensive analysis, we identified 39 genes that were differentially expressed in both patient tissues and cell samples and defined these 39 risk genes as gemcitabine resistance-associated risk genes (Fig. 1A). To explore the possible role of these 39 risk genes in pancreatic cancer while avoiding the limitations of single-database mining, we combined the mRNA expression data of 754 pancreatic cancer tissue samples from the TCGA, E-MTAB-6134 and four GEO datasets (GSE21501, GSE57495, GSE79668, and GSE85916) to form a joint dataset. The SVA package was used to remove batch effects. Principal component analysis (PCA) was used to confirm the effective elimination of batch effects before and after the SVA package was applied (Figs. 1B, 1C). By using the consensus clustering algorithm with the smallest area under the fitting curve and the best clustering effect, we identified two distinct gemcitabine response-related phenotypes (defined as the GR phenotype and GS phenotype) on the basis of these 39 risk genes in the joint dataset (Fig. 1D). The IC50 value of samples with the GR phenotype was significantly greater than that of samples with the GS phenotype (Fig. 1E). Survival analysis of the combined dataset revealed that patients with a GR phenotype had a significantly poorer prognosis than those with a GS phenotype did (Fig. 1F). The same result was also observed in the TCGA cohort (Fig. 1G). In addition, we compared our phenotype with other clinical characteristics via multivariate Cox regression analysis, and our phenotype showed better predictive performance (Fig. 1H). These findings suggest that the gemcitabine response-related phenotype can serve as an independent prognostic factor for pancreatic cancer.

3.2. Distinct inflammatory and immune characteristics between the two gemcitabine response-related phenotypes

Gemcitabine has a cytotoxic effect on cancer cells through the disruption of DNA synthesis, thereby inducing cell apoptosis at the G1 checkpoint [38]. Gemcitabine resistance refers to the ability of pancreatic cancer cells to escape this cytotoxic effect through intrinsic and extrinsic cellular mechanisms [7,8]. The cell-extrinsic mechanism is mainly induced by factors in the TME [39]. The TME of pancreatic cancer is composed of various nontumor cells (such as immune cells, fibroblasts, adipocytes, etc.), an abundant extracellular matrix, and many growth factors and cytokines. In the TME of pancreatic cancer, the dense desmoplastic stroma constitutes a physical barrier to gemcitabine delivery; the accumulation of multiple immune suppressor cells promotes the formation and development of an immunosuppressive microenvironment; and abundant inflammatory factors also play important roles. We therefore analyzed the influences of gemcitabine response-associated genes on the immune microenvironment and on inflammation and chemokines in pancreatic cancer.

As shown in Fig. 2A, a variety of chemokines, such as CXCL13 and its receptors CXCR5, CCL25, and CCR7 (receptors of CCL21), which have been demonstrated in previous studies to be related to the recruitment, aggregation, and infiltration of antitumor immune cells [9–14], were significantly highly expressed in samples with the GS phenotype. In addition, several inflammatory factors and cytokines involved in the inflammatory response and antitumor immunity, such as IL-12, IL-20, IL-23, IL-18, TGFBR3 and IFN [15–17,40,41], also presented increased expression levels in samples with the GS phenotype. These results suggest that the GS phenotype may be closely related to antitumor immunity. Next, seven algorithms (CIBERSORT [23], ssGSEA [24], XCELL [25,26], TIMER [27,28], quanTIseq [29,30], MCPcounter [31] and EPIC [32] were used to assess immune cell infiltration in samples with these two gemcitabine response-related phenotypes. As shown in Fig. 2B, immune cells that promote antitumor activity, such as $CD4^+$ T cells, $CD8^+$ T cells, NK T cells, B cells, NK cells, cytotoxic lymphocytes, and dendritic cells (DCs), presented increased expression in samples with the

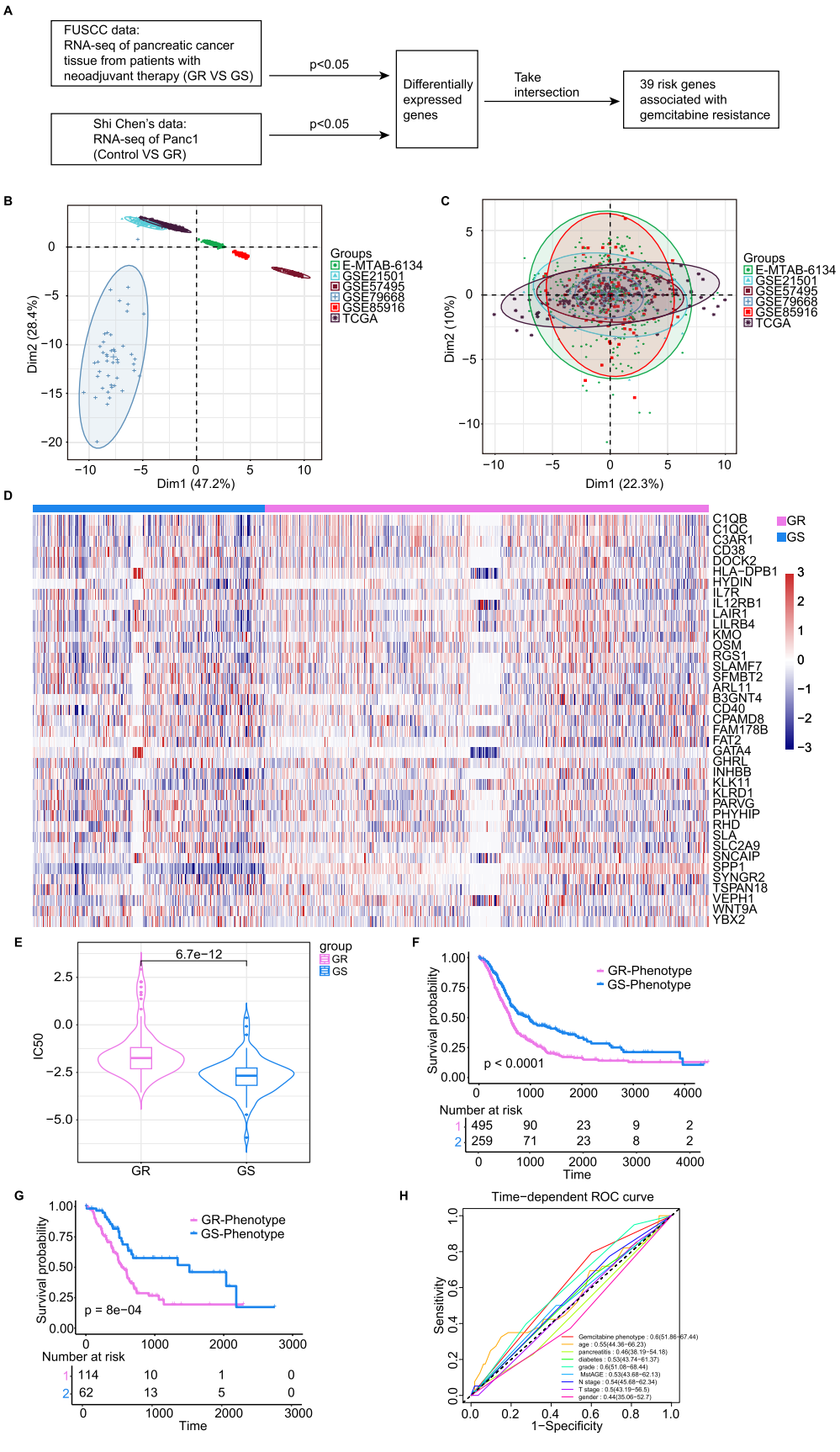

(caption on next page)

Fig. 1. Identification of gemcitabine response related phenotypes by unsupervised clustering. (A) Workflow showing the acquisition of 39 risk genes associated gemcitabine response. (B) The principal component analysis (PCA) plot of the gene expression in six datasets (TCGA, E-MTAB-6134, GSE21501, GSE57495, GSE79668, and GSE85916) before the batch effect removed. (C) The PCA plot of the gene expression in six datasets (TCGA, E-MTAB-6134, GSE21501, GSE57495, GSE79668, and GSE85916) after the batch effect removed. (D) A thermogram showing the expression models of 39 gemcitabine response associated risk genes in two distinct gemcitabine response associated phenotypes (GS-phenotype and GR-phenotype). (E) Assessment of IC50 values of GS-phenotype and GR-phenotype. (F) Survival differences between GS-phenotype and GR-phenotype in the joint cohort. (G) Survival differences between GS-phenotype and GR-phenotype in TCGA cohort. (H) Multivariate Cox regression analysis of our phenotypes and other clinical characteristics. GR, gemcitabine resistant; GS, gemcitabine sensitive.

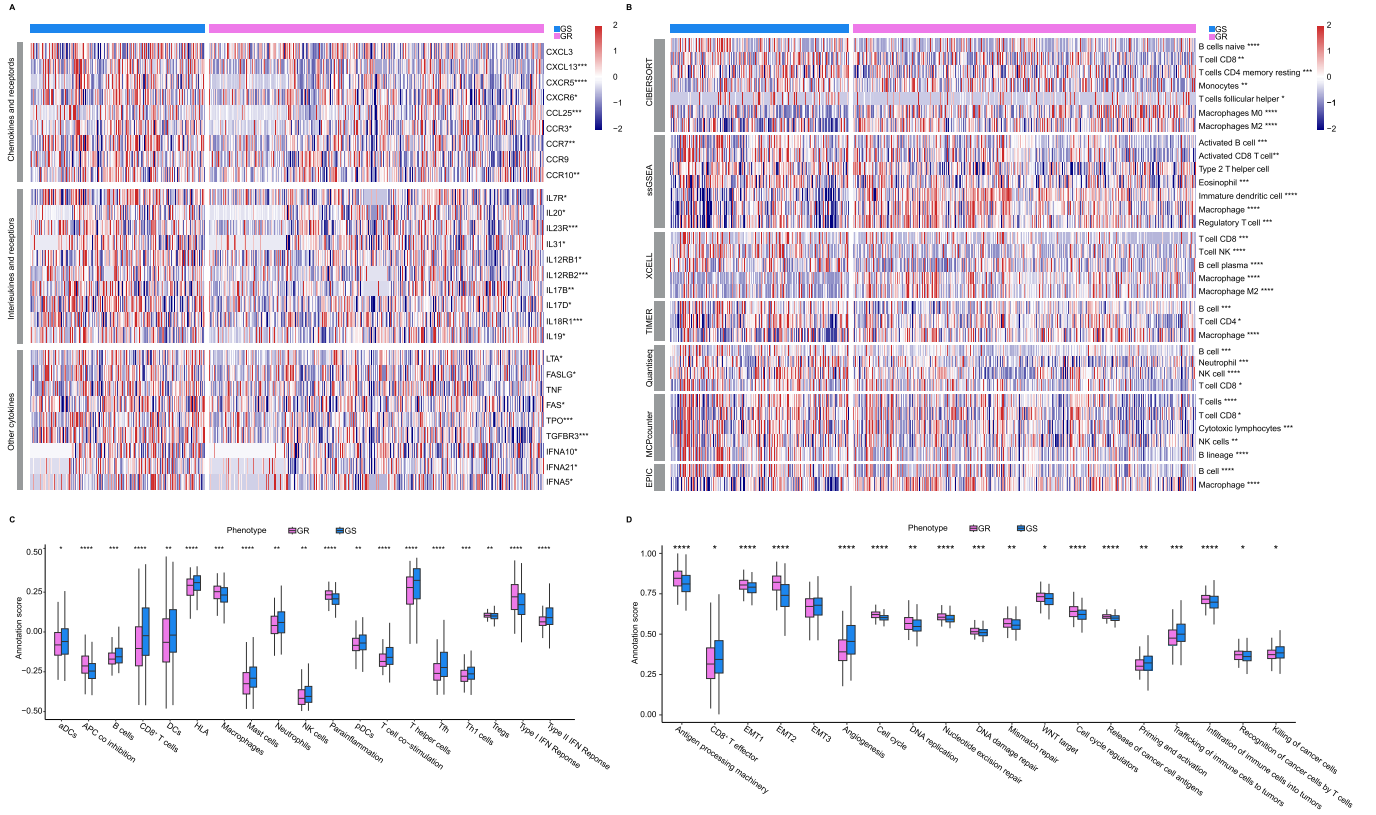

Fig. 2. Different inflammatory and immune characteristics between two gemcitabine response associated phenotypes. (A) The heatmap showing the differences of chemokines and interleukins infiltration between GS-phenotype and GR-phenotype. (B) The heatmap showing the differences of immune cell infiltration between GS-phenotype and GR-phenotype. (C) Differences of immune response related processes between GS-phenotype and GR-phenotype. (D) Differences of tumor progression related signatures between GS-phenotype and GR-phenotype. * $P < 0.05$, * * $P < 0.01$, * ** $P < 0.001$. GR, gemcitabine resistant; GS, gemcitabine sensitive.

GS phenotype. Conversely, the levels of most immunosuppressive immune cells, such as regulatory T cells (Tregs) and M0 and M2 macrophages, were greater in samples with the GR phenotype. Meanwhile, the Estimate algorithm was performed to evaluate the immune-related processes. Consistent with previous results, processes related to the activation of immune responses, including the level of immunoreactive cells (such as CD4 + T cells, CD8 + T cells and B cells) and the levels of antigen-presenting cells (such as DCs), were increased in samples with the GS phenotype. Similarly, the number of immunosuppressive cells was lower in samples with the GS phenotype (Fig. 2C). In addition to gemcitabine resistance caused by extracellular mechanisms, cancer cells can also modify themselves to escape the killing effects of cytotoxic drugs. By evaluating features associated with tumor progression, we found that several characteristics, including epithelial-mesenchymal transition (EMT), DNA damage repair and activation of the WNT signaling pathway, which are endogenous mechanisms that may lead to gemcitabine resistance in cancer cells, were up-regulated in samples with the GR phenotype (Fig. 2D).

3.3. High MLDPP is inversely associated with the survival of pancreatic cancer patients

Next, we constructed a machine learning-derived prognostic profile (MLDPP) to predict the associations between the expression of 39 risk genes associated with the gemcitabine response and the prognosis of pancreatic cancer patients [42,43]. We conducted 10 machine learning algorithms, including random survival forest (RSF), generalized boosted regression modeling (GBM), Ridge, supervised principal component (SuperPC), elastic net (Enet), partial least squares regression for Cox (PlsRcox), CoxBoost, Lasso, and stepwise COX, and used 10-fold cross-validation approaches to generate their 101 combinational algorithms. All the constructed models were evaluated in both the joint cohort and the six single cohorts, and the C-index was calculated to select the optimal signature. As shown in Fig. 3A, the top prediction model out of the 101 models was RSF, which had the highest average C-index (0.6134) across all cohorts; this model showed unparalleled predication ability. Therefore, we identified RSF as a predictive model with high accuracy and translational relevance to identify patients with high/low expression of 39 risk genes. Kaplan—Meier (K–M) survival analysis revealed that in each cohort, including the TCGA ($p < 0.0001$), GSE21501 ($p = 0.033$), GSE57495 ($p = 0.048$), GSE85916

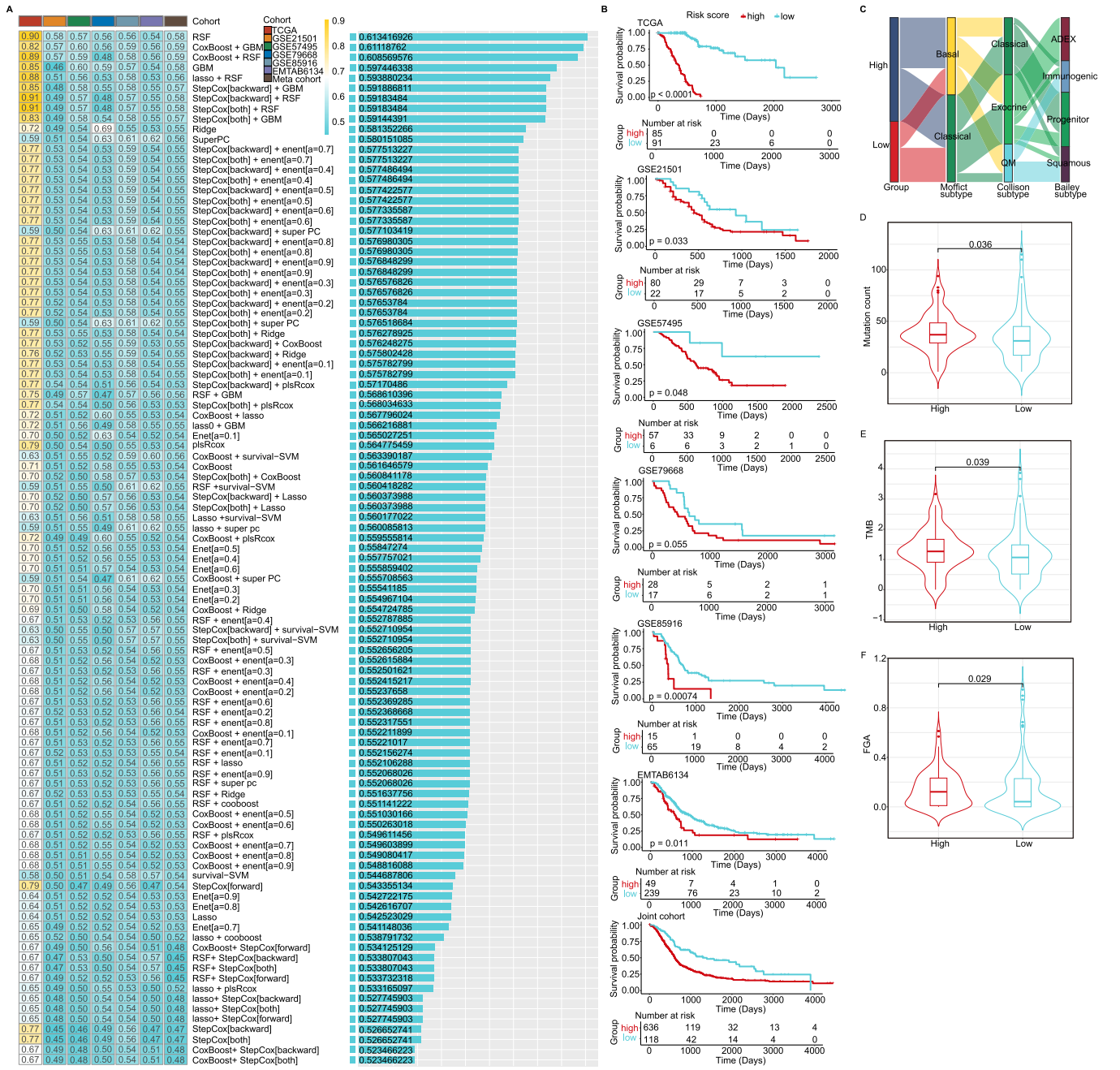

Fig. 3. High MLDPP is inversely correlated with the patient survival in pancreatic cancer. (A) Construction of a machine learning-derived prognostic profile (MLDPP). (B) Kaplan–Meier survival analysis of overall survival between high and low MLDPP groups in TCGA, E-MTAB-6134, GSE21501, GSE57495, GSE79668, GSE85916 and joint cohort. (C) A Sankey diagram showing the correlation between MLDPP group and pancreatic cancer subtype. (D) The difference in mutation count between high and low MLDPP groups. (E) The difference in tumor mutation burden (TMB) between high and low MLDPP groups. (F) The difference in fraction of genome altered (FGA) between high and low MLDPP groups. * $P < 0.05$, * * $P < 0.01$, * ** $P < 0.001$.

($p = 0.00074$), EMTAB6134 ($p = 0.011$) and joint ($p < 0.0001$) cohorts, patients with high MLDPP had significantly lower overall survival than patients with low MLDPP did (Fig. 3B). Although overall survival was not significantly different in the GSE79668 cohort, which may be explained by the small sample size.

Subtype analysis revealed that the basal-phenotype group was mainly composed of high-risk score samples, whereas the classic-subtype group consisted of a similar proportion of samples with high- and low-risk scores [44,45] (Fig. 3C). Analysis of the tumor molecular mutation count, tumor mutation burden (TMB) and fraction of genome altered (FGA) revealed that the above indicators were greater in the high-MLDPP subgroup than in the low-MLDPP subgroup, indicating that high MLDPP is related to a poor prognosis (Fig. 3D, E, F).

3.4. *High expression of gemcitabine response related genes is associated with gemcitabine resistance*

Through Kyoto Encyclopedia of Genes and Genomes (KEGG) enrichment analysis of 1610 differentially expressed genes between the high- and low-MLDPP groups, we found that these differentially expressed genes were enriched mainly in the drug response pathway (Fig. 4A). Therefore, we next explored the relationship between the expression of 39 risk genes and drug sensitivity to multiple chemotherapy agents, including gemcitabine. Using a public

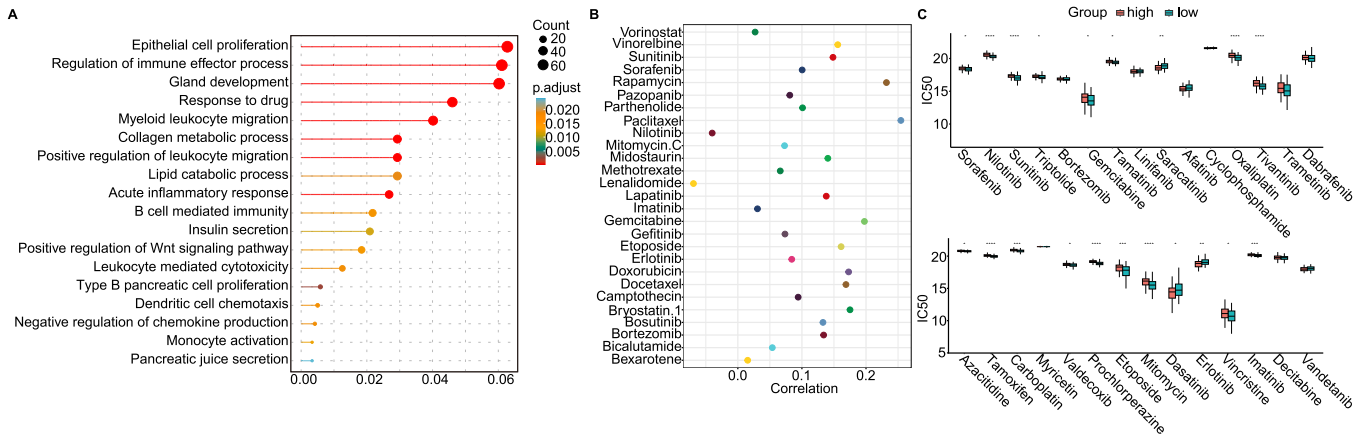

Fig. 4. High MLDPP is positively associated with drug resistance to multiple chemotherapy agents. (A) Kyoto Encyclopedia of Genes and Genome (KEGG) enrichment analysis of differentially expressed genes between high and low MLDPP groups. (B) Correlation between MLDPP and IC50 of chemotherapy drugs (from CGP database). (C) The difference in IC50 values of typical chemotherapy drugs between high and low MLDPP groups (from CTRP database). * $P < 0.05$, * * $P < 0.01$, * ** $P < 0.001$.

pharmacogenomics database (The Cancer Genome Project database), we found that the risk score according to gemcitabine response-associated genes was positively associated with the IC50 values of most chemotherapy drugs and negatively associated with those of a few drugs, including nilotinib and lenalidomide (Fig. 4B). Similarly, drug predictions from the CTRP database yielded similar results. High MLDPP was positively associated with the IC50 values for most chemotherapy agents, including gemcitabine, and negatively associated with only saracatinib and erlotinib (Fig. 4C). These results suggest that a high risk score for gemcitabine response-associated risk genes is correlated with resistance to most chemotherapy drugs, including gemcitabine.

3.5. *Complement C3a is highly expressed and is associated with neoadjuvant chemotherapy resistance in pancreatic cancer*

Gemcitabine response-associated risk genes are related to gemcitabine resistance and immune infiltration. By taking the intersection of differentially expressed genes associated with the gemcitabine response, immune cell infiltration (Table S2) and the IC50 value (Table S3), we identified their mutual differential genes as *C3aR1*, the receptor of complement C3a (Fig. 5A, S2A, S2B). C3a is the end product of the complement system activation [46,47]. The complement system, considered a cornerstone of innate immunity, is composed of more than 30 proteins and plays a key role in maintaining host homeostasis, participating in inflammation processes and defending against pathogen invasion. The classical pathway, alternative pathway and lectin pathway are the three main pathways of complement activation. Although these three pathways are initiated by different mechanisms, the cleavage of C3 into the active fragments C3a and C3b via C3 invertase-mediated catalysis is a common process. C3b eventually catalyzes the formation of another important anaphylatoxin fragment, C5a. C3a binds to its receptor C3aR (gene: *C3AR1*), which has been shown to play important roles in several pathophysiological processes, such as inducing chronic inflammation, to shape the immunosuppressive microenvironment, and participate in tumor angiogenesis [48,49].

In the previous process, we identified *C3aR1* and analyzed its roles mainly through the analysis of data associated with gemcitabine resistance in pancreatic cancer; we hope to continue to explore the role of complement C3a and its receptor in this respect in our next studies By exploiting the TCGA database (pancreatic cancer), we found that high expression of *C3aR1* is associated with a poor prognosis for pancreatic cancer (Fig. 5B). Analysis of clinical sample data from the Gene Expression Profiling Interactive Analysis (GEPIA) online database also revealed that *C3aR1* expression was significantly elevated in pancreatic cancer tissue compared with normal pancreatic tissue (Fig. 5C). We subsequently analyzed the levels of complement C3, C3a, and C3aR in 46 pairs of pancreatic cancer and adjacent normal pancreatic tissues from our center via IHC staining. As shown in Fig. 5D, the expression levels of C3, C3a, and C3aR in pancreatic cancer were significantly greater than those in adjacent normal pancreatic tissues, indicating the activation of the complement system during the progression of pancreatic cancer. C3a and its receptor C3aR are abnormally highly expressed in pancreatic cancer. ELISA of 16 pairs of pancreatic cancer and adjacent normal pancreatic tissues from pancreatic patients at our center also revealed increased C3a expression in tumor tissue (Fig. 5F). Moreover, 10 pancreatic cancer tissues from *LSL-Kras*$^{G12D/+}$*LSL-Trp53*$^{R172H/+}$*Pdx-1-Cre* (KPC) mice and 10 normal pancreatic tissues from wild-type C57BL/6 J mice were collected for H&E staining and IHC staining. Data from mice also revealed that C3a/C3aR expression was upregulated in pancreatic cancer (Fig. 5E). IHC and ELISA experiments revealed that C3a/C3aR was abnormally highly expressed in human and mouse pancreatic cancer tissues.

To further investigate the prognostic value of C3a/C3aR expression in pancreatic cancer, 83 pancreatic cancer tissues from patients in our center were collected to generate a tissue microarray (TMA). The expression level of C3aR was detected via IHC staining. Patients were divided into a high-C3aR expression group (n = 39) and a low-C3aR expression group (n = 44) according to their IHC score (Fig. 5G, S3). Patients in the high C3aR expression group had significantly shorter survival (median: 462 days vs. 818 days, respectively; log-rank test, P = 0.0023; Fig. 5H). This finding is consistent with the results from the TCGA database, indicating that high expression of C3aR in pancreatic cancer is significantly associated with a poor prognosis.

We further investigated whether the expression of C3aR is related to the poor efficacy of gemcitabine neoadjuvant therapy for pancreatic cancer. By performing IHC staining and ELISA, we detected the expression of C3a and C3aR in 14 pairs of tumor tissues collected from pancreatic cancer patients who were resistant or sensitive to gemcitabine neoadjuvant therapy. The results revealed that the C3a/C3aR expression levels were significantly greater in the tumor tissues of the GR patients than in those of the GS patients (Fig. 5I, J). Moreover, we analyzed the correlations between C3a expression and the clinicopathologic features of 71 pancreatic cancer patients ccunderwent neoadjuvant therapy (Table 1). We found that high C3a expression was positively related to more extensive microvascular invasion, larger tumor volume, increased lymph node metastasis, more advanced tumor stage and higher serum CA19–9 levels. Collectively, these results suggest that C3a/C3aR is highly expressed in pancreatic cancer and is associated

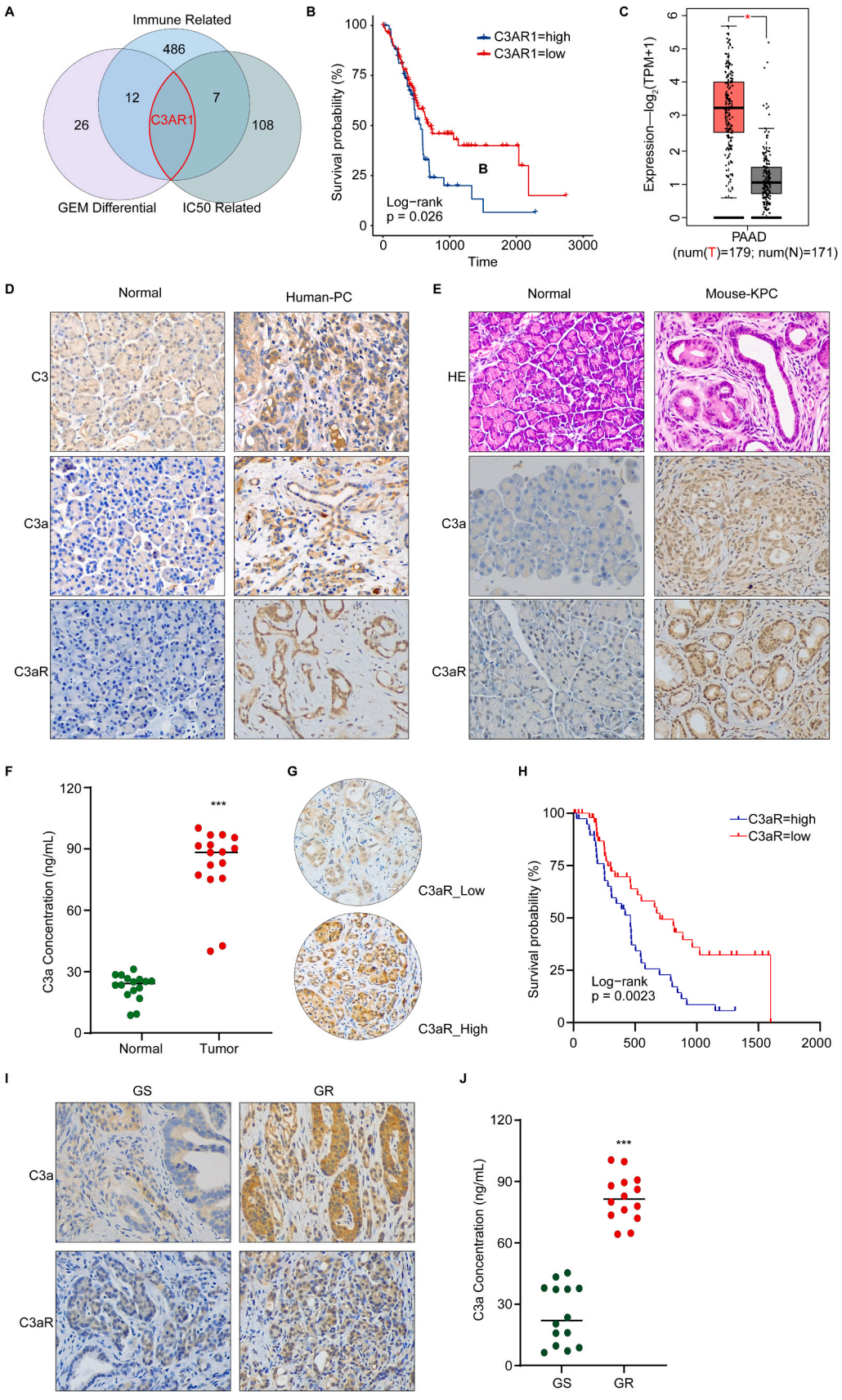

(caption on next page)

Fig. 5. Complement C3a is highly expressed and is associated with neoadjuvant chemotherapy resistance in pancreatic cancer. (A) Venn diagram, including 3 parts of data: (1) differential genes associated with distinct gemcitabine response (in purple color); (2) differential genes associated with distinct immune infiltration (in blue color); (3) differential genes associated with distinct IC50 value of gemcitabine (in gray color). C3aR1 was the only differential gene shared by all these three parts. (B) Analysis of clinical samples from TCGA(PAAD) database showed that high expression of C3aR1 was associated with poor survival in pancreatic cancer. (C) The boxplot showing the differential expression of C3aR1 in pancreatic cancer tissue (T) and normal pancreatic tissue (N). (D) Representative IHC staining images showed the differential expression of C3, C3a, and C3aR in normal pancreatic tissue and human pancreatic cancer. (E) Representative images of H&E staining and IHC staining showed the differential expression of C3a, and C3aR in normal pancreatic tissue from wild-type (WT) C57BL/6 J mice and in pancreatic cancer tissue from KPC mice. (F) C3a protein levels in human pancreatic cancer tissue and adjacent normal pancreatic tissue were accessed by ELISA. (G) Representative IHC staining images of high/low C3aR expression in pancreatic cancer tissue from FUSCC-TMA. (H) Kaplan–Meier survival analysis of overall survival between high and low C3aR groups in FUSCC-TMA samples. (I) Representative IHC staining images showed the differential expression of C3a and C3aR in pancreatic cancer tissue from gemcitabine-sensitive (GS) patients and gemcitabine-resistant patients. (J) C3a protein levels in pancreatic cancer tissue from GS/GR patients were accessed by ELISA. * $P < 0.05$, * * $P < 0.01$, * ** $P < 0.001$. GEM, gemcitabine.

Table 1
Relationship between C3a expression and clinicopathological characteristics of pancreatic cancer patients underwent neoadjuvant therapy.

Characteristics	C3a Expression		P Value
	Low C3a Group (n = 39)	High C3a Group (n = 32)	
Age (years)			0.621
≤ 60	16	15	
> 60	23	17	
Gender			0.267
Male	18	19	
Female	21	13	
BMI (kg/m2)			0.877
≤ 23	19	15	
> 23	20	17	
Tumor location			0.817
Head and neck	16	14	
Body and tail	23	18	
Neural invasion			0.226
Yes	33	30	
No	6	2	
Microvascular invasion			0.033
Yes	11	17	
No	28	15	
Tumor differentiation			0.935
Poor	11	8	
Moderate	23	15	
Well	4	4	
8th AJCC stage			0.038
I	21	10	
II	13	10	
III	5	12	
8th T stage			0.034
I	18	7	
II	13	10	
III	8	15	
8th N stage			0.044
N0	21	14	
N1	13	6	
N2	5	12	
Preoperative CA19 −9			0.047
≤ 37	11	3	
> 37	28	29	
Response to Gemcitabine			< 0.001
GR	9	26	
GS	30	6	

with a poor prognosis and poor efficacy of neoadjuvant therapy.

3.6. Activation of the C3a/C3aR pathway promotes the malignant phenotype of pancreatic cancer cells and induces gemcitabine resistance

To explore the possible role of the C3a/C3aR pathway in pancreatic cancer cells, we cultured and treated Panc-1 cells with different concentrations of recombinant C3a protein to observe the proliferation and migration of the cells, and PBS was used as a negative control. Western blotting revealed that the expression level of C3aR1 in Panc-1 cells was increased after treatment with recombinant C3a protein (Fig. 6A). As shown in Figs. 6B and 6C, the results of the EdU assays revealed that the proliferation ability of Panc-1 cells was significantly increased after 48 h of C3a treatment. Transwell assays revealed an obvious increase in the migration ability of Panc-1 cells (Fig. 6D, E). These results suggest that the activation of the C3a/C3aR pathway enhances the proliferation and migration of Panc-1 cells in a concentration-dependent manner. The analysis of IC50 values also revealed that C3a/C3aR pathway activation led to a decrease in the gemcitabine sensitivity of Panc-1 cells (Fig. 6F). The same phenomenon was observed when mouse Panc-02 cells were stimulated with different concentrations of recombinant mouse C3a. As shown in Fig. 6G, after treatment with recombinant C3a protein (mouse), the expression level of C3aR1 in Panc-02 cells was increased. C3a (mouse) promoted the proliferation (Fig. 6 H, I) and migration ability of Panc-02 cells (Fig. 6J, K), and decreased their sensitivity to gemcitabine (Fig. 6L). Taken together, these results suggested that C3a activated pancreatic cancer cells, which increased their proliferation and migration ability in vitro and promoted cell resistance to gemcitabine.

3.7. Knockdown of C3aR does not affect the progression-related behaviors of pancreatic cancer cells in vitro

Next, we knocked down C3aR expression in pancreatic cancer cell lines, including Panc-1 cells and Panc-02 cells, to investigate the accompanying effects on the malignant biological phenotype of pancreatic cancer cells. Panc-1/Panc-02 cells were infected with a lentivirus expressing C3aR-specific shRNA, and a scrambled shRNA was used as a control. As shown in Fig. 7A, Western blotting results confirmed the successful generation of the Panc-1 cell line with C3aR knockdown. Control cells (sh-Scr) and C3aR-deficient cells (sh#1, sh#2) were seeded into 96-well plates at a density of 5000 cells per well, and the optical density at 450 nm of each group at 0, 1, 2, 3, and 4 days was detected via the CCK-8 assay. The results showed that C3aR knockdown did not significantly affect the proliferative capacity of Panc-1 cells (Fig. 7B). The EdU assay also yielded consistent results (Fig. 7C, D). In addition, Transwell assays revealed that the migration ability of Panc-1 cells did not change as well in C3aR-deficient Panc-1 cells (Fig. 7E, F). A similar phenomenon was also observed in Panc-02 cells. Western blotting verified the successful generation of Panc-02 stable stains with deficient C3aR expression (Fig. S4A). CCK-8 (Fig. S4B) and EdU (Fig. S4C, S4D) assays revealed that the proliferation ability of Panc-02 cells was not affected by C3aR deficiency. The results of the Transwell assay revealed that the migration capacity of Panc-02 cells was also unaffected (Fig. S5E, S5F).

We subsequently treated Panc-1 cells with 500 ng/ml recombinant C3a protein to explore whether C3aR knockdown affects the proliferation and migration ability of pancreatic cancer cells stimulated with C3a. Under stimulation with a certain concentration of C3a, qPCR revealed increased expression of C3aR in control cells to a certain extent, whereas no similar increase was observed in C3aR-knockdown Panc-1 cells (Fig. 7G). EdU (Fig. 7H, I) and Transwell (Fig. 7J, K) assays also revealed that the proliferation and migration abilities of the control cells

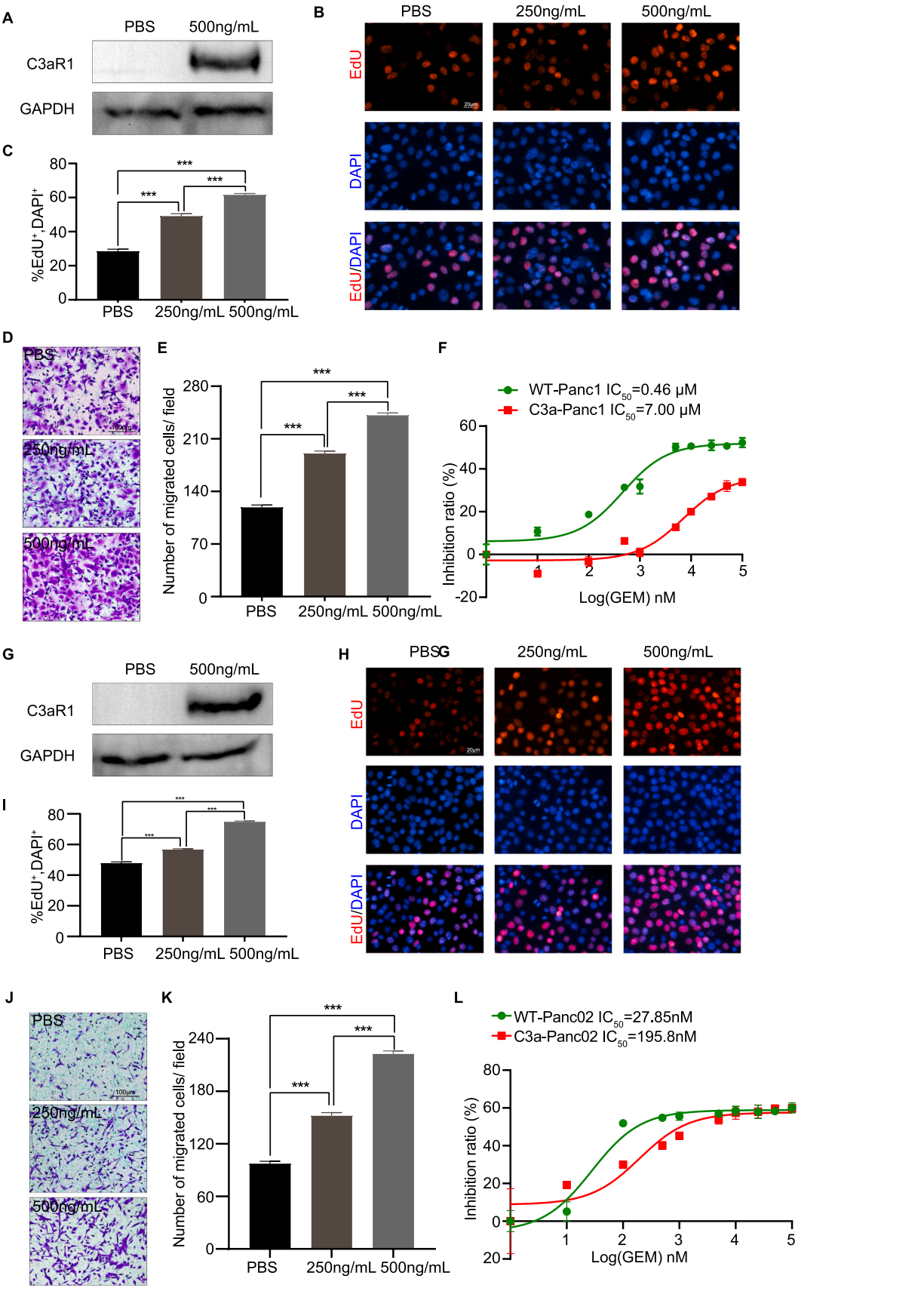

(caption on next page)

Fig. 6. The activation of C3a/C3aR pathway promotes the proliferation, migration and gemcitabine resistance in pancreatic cancer cells. (A) Western blotting was used to detect the C3aR expression in Panc-1 cells treated with PBS or 500 ng/ml recombinant C3a protein. (B) Representative images of EdU assays showed that C3a recombinant protein promotes the proliferation of Panc-1 cells in a concentration-dependent manner. (C) The bar plot showed the percentage of EdU^+ cells per field. (D) Representative images of Transwell assays showed that C3a recombinant protein promotes the migration of Panc-1 cells in a concentration-dependent manner. (E) The bar plot showed the percentage of migrated cells per field. (F) CCK-8 assay showed that C3a recombinant protein increased the IC50 values of Panc-1 cells to gemcitabine. (G) Western blotting was used to detect the C3aR expression in Panc-02 cells treated with PBS or 500 ng/ml recombinant C3a protein (mouse). (H) Representative images of EdU assays showing that C3a recombinant protein (mouse) promotes the proliferation of Panc-02 cells in a concentration-dependent manner. (I) The bar plot showed the percentage of EdU^+ cells per field. (J) Representative images of Transwell assays showing that C3a recombinant protein (mouse) promotes the migration of Panc-02 cells in a concentration-dependent manner. (K) The bar plot showed the percentage of migrated cells per field. (L) CCK-8 assay showed that C3a recombinant protein (mouse) increased the IC50 values of Panc-02 cells to gemcitabine. * $P < 0.05$, * * $P < 0.01$, * ** $P < 0.001$. GEM, gemcitabine.

increased under the condition of complement C3a protein treatment, whereas those of the C3aR-deficient Panc-1 cells did not change. Similarly, in Panc-02 cells, C3aR was knocked down, and the cells were subsequently treated with 500 ng/ml recombinant C3a protein (mouse). However, C3aR expression in C3aR-deficient cells did not increase (Fig. S4G), and the proliferation (Fig. S4H, S4I) and migration (Fig. S4J, S4K) abilities of the cells did not increase. These results suggest that C3a binds to and acts on its receptor C3aR on the cell membrane, promoting the malignant phenotype of pancreatic cancer cells. However, in vitro, C3aR knockdown did not affect the proliferation or migration capacity of pancreatic cancer cells.

Female BALB/c-nu mice aged 5 weeks were randomly divided into 2 groups and injected with control Panc-1 cells or C3aR-deficient cells to construct a subcutaneous tumor model. The tumor volume was observed and recorded every 3 days, and the tumors were separated and collected on the 21st day of treatment. We found that tumor progression in the C3aR-deficient group (shRNA) was slower than that in the control group (sh-Scr) under in vivo conditions (Fig. 7L, M). The successful knockdown of C3aR was demonstrated by Western blotting of tumor tissue (Fig. 7N). In addition, ELISA detection of C3a expression revealed that the C3a level in the tumor tissues of these two groups of mice was similar (Fig. 7O). These results indicate that under continuous stimulation with C3a in vivo, C3aR knockdown suppresses tumor growth and progression. Immunofluorescence staining of Ki-67 in tumor tissue sections also revealed that the proportion of proliferating cancer cells in the C3aR-deficient group was significantly lower than that in the control group under in vivo conditions (Fig. 7P, Q). Consistent results were also observed in a subcutaneous tumor model constructed with control Panc-02 cells and C3aR-deficient Panc-02 cells; tumor growth was significantly inhibited when C3aR was knocked down (Fig. S4L, S4M). Western blotting verified the successful knockdown of C3aR (Fig. S4N).

These results suggest that the C3a/C3aR pathway may be a potential target for the treatment of pancreatic cancer. Targeting the C3a/C3aR signaling pathway may provide direction for the treatment of pancreatic cancer.

3.8. A C3aR antagonist (SB290157) attenuates the effects of C3a activation in pancreatic cancer

SB290157 is a well-known effective and selective antagonist of C3aR and has been widely used in basic and preclinical C3a studies to block the interaction between C3a and C3aR [50]. In a mouse model, SB290157 was shown to inhibit breast cancer lung metastasis by blocking C3a-C3aR signaling [51]. Similarly, in mouse medulloblastoma, SB290157 has also been shown to inhibit tumor progression by restraining astrocyte activation [52]. Therefore, we next investigated whether the C3aR antagonist SB290157 could counter the cancer-promoting effect of C3aR activation in pancreatic cancer cells. EdU assays revealed that the addition of C3a to the cell supernatant for 48 h stimulated Panc-1 cell proliferation. However, this enhancement effect was significantly countered by the addition of SB290157, and Panc-1 cell proliferation was inhibited (Fig. 8A, B). Transwell assays also revealed that the increased migration ability of Panc-1 cells induced by C3aR signal activation was significantly inhibited by SB290157 (Fig. 8C, D). Similarly, the resistance of Panc-1 cells to gemcitabine induced by C3aR signaling was attenuated by SB290157 (Fig. 8E). Similarly, SB290157 treatment weakened the proliferation (Fig. S5A, S5B), migration (Fig. S5C, S5D) and gemcitabine resistance (Fig. S5E) induced by C3a/C3aR activation in Panc-02 cells.

To assess whether SB290157 can also counter the tumor-promoting effects of C3aR signaling activation in pancreatic cancer in vivo, we constructed a mouse subcutaneous tumor model using Panc-1 cells. BALB/c-nu mice were randomly divided into 4 groups. The mice were respectively treated with 20 mg/kg gemcitabine, 20 mg/kg SB290157, 20 mg/kg gemcitabine combined with 20 mg/kg SB29015 by intraperitoneal injection once a day, with 3 % DMSO in MCT as the vehicle. An equal volume of MCT was used as a negative control. By measuring and recording changes in tumor volume, we found that the tumor volume continued to increase in the control group, while gemcitabine treatment significantly delayed this progression (Fig. 8F). Interestingly, as a well-known antagonist of C3aR, SB290157 has an almost equal ability to inhibit pancreatic tumor progression as gemcitabine does. Encouragingly, the combination of gemcitabine and SB290157 had a significantly better effect than either treatment alone. On the 14th day of treatment, the tumors were separated, collected and photographed for size evaluation (Fig. 8G). Frozen sections were prepared, and IF staining of Ki-67 and cleaved caspase 3 (CC3) proteins was performed to detect the proliferation and apoptosis of tumor cells. Compared with the control treatment, treatment with gemcitabine or SB290157 markedly attenuated the proliferation (Fig. 8H, I) and promoted the apoptosis in Panc-1 cells (Fig. 8J, K). The effect was more pronounced in the mice treated with the combination of the two drugs. A similar phenomenon was also observed in a mouse subcutaneous tumor model constructed with Panc-02 cells (Fig. S5F, S5G). The above in vitro and in vivo experiments showed that pharmacological inhibition of C3aR signaling can significantly suppress pancreatic cancer cell proliferation, migration and drug resistance both in vivo and in vitro.

4. Discussion

Pancreatic cancer is one of the most lethal malignant cancers threatening human health and places a considerable burden on the economy and societycc [2]. In recent years, the incidence and mortality rates of pancreatic cancer have increased annually worldwide. Currently, it is the third leading cause of cancer-related death in the United States and is expected to become the second leading cause of cancer-related death in Western countries in the near future [1,3]. Surgery and chemotherapy are the main treatment options for pancreatic cancer. However, owing to extensive distant metastasis, only approximately 15–20 % of patients are eligible for surgery at the first diagnosis [4,53]. The widespread occurrence of chemotherapy resistance also presents great challenges for the treatment of pancreatic cancer. Gemcitabine is an important first-line chemotherapy drug, but its response rate is only approximately 20 % [5,6]. Our study aimed to explore the potential mechanism of gemcitabine chemotherapy resistance in pancreatic cancer to reveal potential targets for pancreatic cancer treatment.

By performing a comprehensive analysis of RNA sequencing data

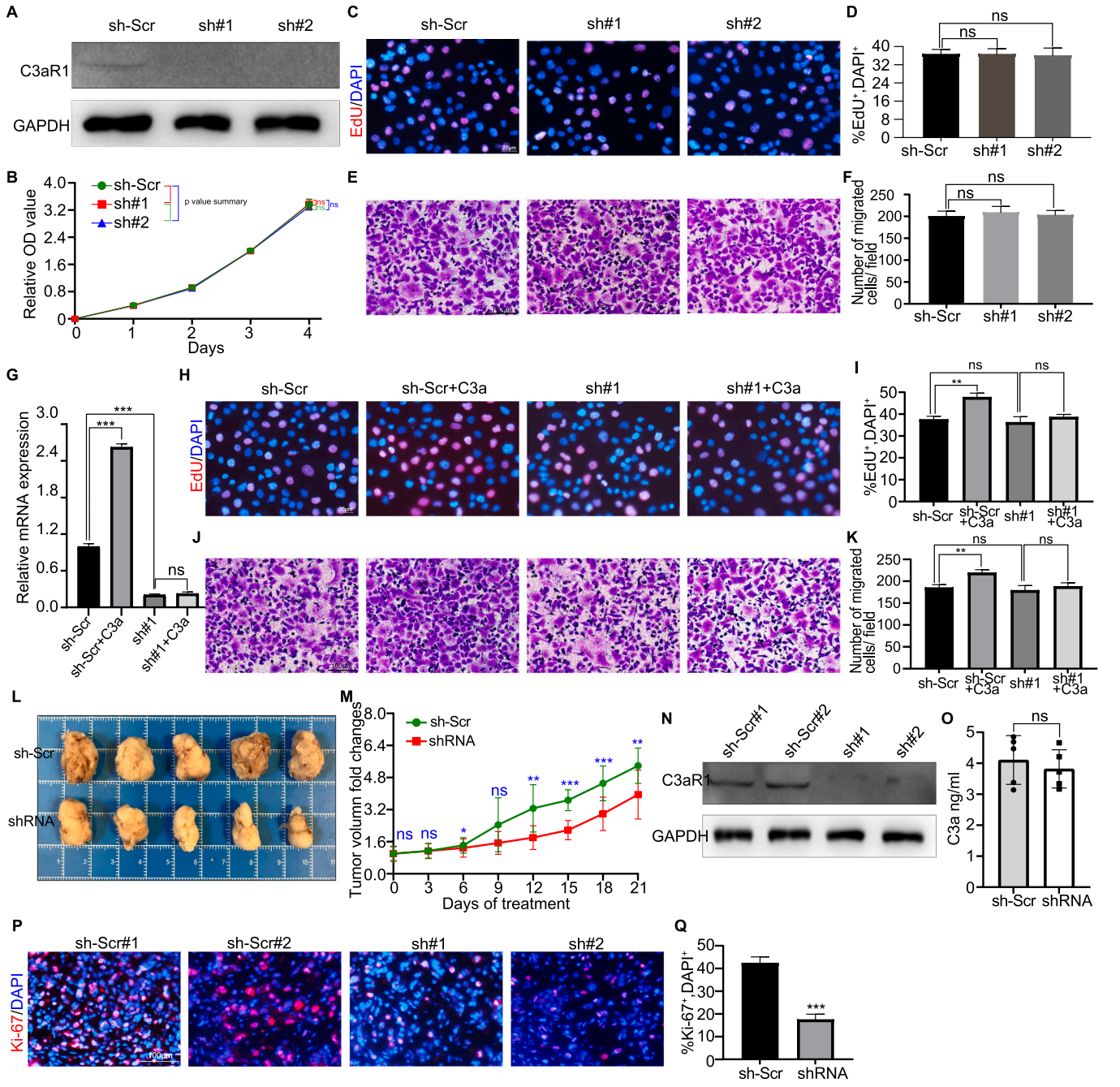

Fig. 7. Knockdown of C3aR does not affect the progression of pancreatic cancer cells in vitro. A.A-F Panc-1 cells were infected with C3aR shRNA to knock down the C3aR expression (sh#1, sh#2), or infected with a scrambled shRNA as the control group (sh-Scr). (A) Western blotting was used to detect C3aR expression in control cells and C3aR-deficient cells to evaluate the transfection efficiency. (B) CCK8 assay was used to evaluate the cell proliferation, and the relative optical density of each group at day 0, 1, 2, 3 and 4 was measured. The line chart showed that C3aR knockdown did not change the proliferation capacity of Panc-1 cells. (C) Representative images of EdU assays showed that the knockdown of C3aR did not affect the proliferation capacity of Panc-1 cells. (D) The bar plot showed the percentage of EdU^+ cells per field. (E) Representative images of Transwell assays showed that the knockdown of C3aR did not affect the migration ability of Panc-1 cells. (F) The bar plot showed the percentage of migrated cells per field. G-K C3aR-deficient Panc-1cells or control cells were treated with C3a recombinant protein at a concentration of 0 or 500 ng/ml. (G) RT-qPCR was used to detect the C3aR expression in control cells and C3aR-deficient cells with or without C3a treatment. (H) Representative images of EdU assays showed that the proliferation ability of control cells enhanced under the C3a treatment, while that of C3aR-deficient Panc-1 cells did not change. (I) The bar plot showed the percentage of EdU^+ cells per field. (J) Representative images of Transwell assays showed that the migration ability of control cells enhanced under the C3a treatment, while that of C3aR-deficient Panc-1 cells did not change. (K) The bar plot showed the percentage of migrated cells per field. L-O Ten female BALB/c-nu mice were randomly divided into 2 groups and respectively injected with control Panc-1 cells and C3aR-deficient cells to construct subcutaneous tumor model. Tumor volume was observed and recorded every 3 days. (L) Line charts of volume changes of subcutaneous tumor. (M) On the 21st of treatment, subcutaneous tumors were separated to show tumor size. (N) Western blotting was used to detect the expression of C3aR in subcutaneous tumors. (O) Elisa was used to detect the expression of complement C3a in subcutaneous tumors. (P) Frozen sections were prepared from tumor tissues. IF staining with antibodies to Ki-67 (in red color) was performed to detect proliferation of Panc-1 cells, and DAPI was used to counterstain the cell nuclei (in blue color). (Q) The bar plot showed the percentage of $Ki\text{-}67^+$ cells per field.

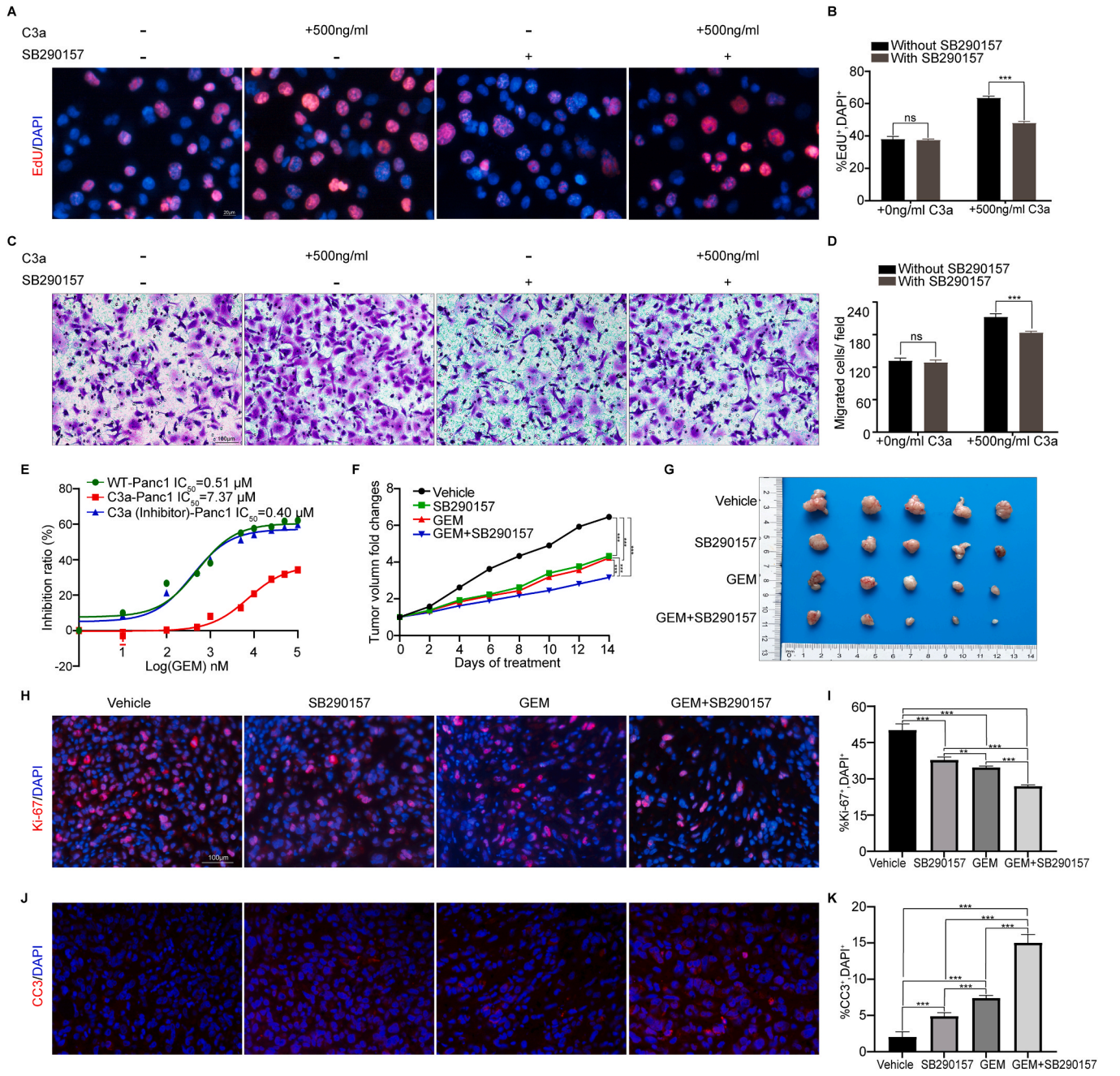

Fig. 8. C3aR antagonist (SB290157) attenuated the effects of C3a activation in pancreatic cancer. (A) Representative images of EdU assays showed that the treatment of SB290157 attenuated C3a-induced proliferation in Panc-1 cells. (B) The bar plot showed the percentage of EdU^+ cells per field. (C) Representative images of Transwell assays showed that the treatment of SB290157 attenuated C3a-induced migration in Panc-1 cells. (D) The bar plot showed the percentage of migrated cells per field. (E) CCK-8 assay showed that the treatment of SB290157 attenuated C3a-induced gemcitabine resistance in Panc-1 cells. F-K A mouse subcutaneous tumor model of Panc-1 cells was constructed. The mice were randomly grouped and treated with vehicle, 20 mg/kg gemcitabine, 20 mg/kg SB290157, 20 mg/kg gemcitabine combined with 20 mg/kg SB29015 by intraperitoneal injection once a day. (F) Line charts of volume changes of subcutaneous tumor. (G) On the 14th day of treatment, subcutaneous tumors were separated to show tumor size. Frozen sections were prepared from tumor tissues. IF staining with antibodies to Ki-67 (in red color, (H)) and CC3 (in red color, (J)) was performed to detect proliferation and apoptosis of Panc-1 cells. And the percentage of Ki-67^+ cells (I) or $CC3^+$ cells (K) per field was shown by bar plots. * $P < 0.05$, * * $P < 0.01$, * ** $P < 0.001$. GEM, gemcitabine.

from both cell samples and patient samples, we identified 39 risk genes associated with gemcitabine resistance. Then, consensus cluster analysis was used to identify two distinct gemcitabine-responsive phenotypes, namely, the GR phenotype and the GS phenotype, and samples with these two phenotypes exhibited differences in inflammatory and immune characteristics. Next, we constructed a machine learning-derived prognostic profile using 10 machine learning algorithms and their 101 combinations and demonstrated that high gemcitabine risk gene expression is associated with a poor prognosis, high tumor mutation burden, and resistance to multiple chemotherapy drugs, including gemcitabine.

Our study ultimately focused on the receptor for complement C3a, C3aR (gene *C3aR1*), which was the only gene in our analysis that was differentially expressed in both the gemcitabine response and the immune infiltration process. C3a is the final product of complement system activation. In a variety of tumors, C3a is thought to be involved in tumor

occurrence and development [51,54]. For example, in mouse medulloblastoma, C3a is thought to activate astrocytes and promote tumor progression via the production of TNF-α [52]. In human colorectal cancer, serum C3a levels are significantly elevated and are considered an emerging biomarker for colorectal cancer screening tests [55]. In ovarian cancer, C3a decreases the expression of E-cadherin in ovarian cancer cells, thereby promoting the EMT of cancer cells [56]. However, there have not been any concrete studies on whether complement C3a is involved in the progression of pancreatic cancer. In our research, through database mining and sample analysis, we found that C3a/C3aR expression is abnormally high in pancreatic cancer patients and is associated with shorter survival. Higher levels of C3a/C3aR expression in tumor tissues were still positively associated with a poor response to gemcitabine neoadjuvant therapy in patients with pancreatic cancer. A series of functional experiments revealed that C3a binds to and acts on its receptor C3aR on the cell membrane. The activation of C3a/C3aR signaling promoted the proliferation and migration of pancreatic cancer cells and enhanced gemcitabine resistance. In the absence of C3a stimulation in vitro, the knockdown of C3aR did not affect biological characteristics such as the proliferation and migration of pancreatic cancer cells. However, in the presence of continuous C3a stimulation in vivo, the knockdown of C3aR led to significant restriction of tumor growth. This finding is consistent with a previous study reported by Aykut et al. showing that knocking down C3aR in tumor cells can protect against pancreatic tumor growth in vivo [57]. In addition, the C3aR antagonist SB290157 effectively counteracted these cancer-promoting effects both in vitro and in vivo. Our study reveals the cancer-promoting effects of the C3a/C3aR signaling pathway on pancreatic cancer progression, suggesting that the C3a level can be used as a potential biomarker for pancreatic cancer prognosis evaluation. In addition, the C3a/C3aR signaling pathway may be a possible therapeutic target for pancreatic cancer. Our study also demonstrated the good efficacy of the C3aR antagonist SB290157 in inhibiting pancreatic cancer progression and indicated that the combination of gemcitabine and SB290157 may have better efficacy than monotherapy, providing a new possible regimen pancreatic cancer chemotherapy.

The cancer-promoting role of the C3a/C3aR axis in pancreatic cancer has been explored in previous studies. Research by Suzuki et al. revealed that C3a promotes pancreatic cancer cell proliferation, migration, and invasion in vitro, corroborating some findings of our study [58]. Additionally, Sodji et al. reported that C3aR antagonists delayed the growth of pancreatic tumors in murine models, and the combination of these antagonists and radiotherapy yielded enhanced therapeutic effects [59]. These preliminary studies offer valuable insights for our research. At present, the availability of chemotherapeutic drugs is limited, and they are associated with severe side effects. Consequently, there is an urgent need to solve the problem of drug resistance in chemotherapy and to strive for the development of targeted therapeutic drugs with high efficacy and low toxicity. The complement system serves as a pivotal link between innate and adaptive immunity. In cancer, however, the activation of the complement pathway is often perceived to do more harm than good, primarily due to the chemoresistance caused by anaphylatoxins [60]. Research indicates that anaphylatoxins, such as C3a and C5a, may influence the TME by increasing the expression of inflammatory mediators and cytokines or triggering various signaling cascades, such as the PI3K/AKT and C-MET cascades, thereby contributing to cancer progression and chemoresistance [61,62]. In pancreatic cancer, gemcitabine is associated with the occurrence of thrombotic microangiopathy, and the complement inhibitor eculizumab is effective in treating gemcitabine-induced thrombotic microangiopathy [63,64]. However, the concrete role of the C3a/C3aR pathway in gemcitabine resistance in pancreatic cancer remains unexplored. In addition to the finding that the activation of the C3a/C3aR signaling pathway enhances the malignant behaviors of pancreatic cancer cells, such as proliferation and migration, our study further revealed that this activation is associated with increased resistance to gemcitabine. The C3aR antagonist SB290157 neutralized the effects of C3a, and its combination with the chemotherapeutic agent gemcitabine increased treatment efficacy. By using public databases, patient samples, and a series of in vitro and in vivo experiments, we comprehensively demonstrated that complement C3a may act as a bypass pathway to increase therapeutic resistance to gemcitabine in pancreatic cancer from the perspective of complement system activation. Moreover, we confirmed the therapeutic potential of the C3aR1 inhibitor SB290157 in pancreatic cancer using a mouse model; notably, no significant toxic side effects were observed, suggesting that this is a promising targeted clinical treatment strategy.

Unfortunately, our study has not yet revealed the specific mechanism of action of the C3a/C3aR signaling pathway. Previous studies may provide some hints. By evaluating features associated with tumor progression, we found that the process of EMT was significantly greater in samples with the GR phenotype. In a previous study of ovarian cancer, C3a was shown to promote EMT by inhibiting the production of E-cadherin, which was consistent with our findings [56]. Therefore, activation of the C3a/C3aR signaling pathway may promote gemcitabine resistance in pancreatic cancer by promoting the EMT process, and further studies are needed in the future. Regrettably, we measured E-cadherin expression in C3a-treated Panc-1 cells via real-time quantitative PCR and found that it was not decreased after activation of the C3a/C3aR signaling pathway (data not shown). More EMT-related indicators (such as N-cadherin, vimentin, and Twist) need to be detected in further studies [65,66]. Moreover, our study did not reveal the specific source of the abnormally high expression of C3a in pancreatic cancer. As significant disease processes, when malignant tumors are recognized, complement proteins in tissues and fluids may be activated through a variety of complex mechanisms [67–69]. Further investigation of the source and activation pathway of the complement system in pancreatic cancer is also important for subsequent targeted treatment measures. Notably, the abnormally elevated C3a level in tumor tissue is most likely due to increased C3a in circulation. Therefore, knocking out the C3a receptor in pancreatic cancer cells may be the most promising treatment. The construction of a C3aR-deficient KPC mouse model may help to verify our hypothesis, and further efforts are needed to address these questions.

In conclusion, our study revealed 39 risk genes associated with gemcitabine resistance in pancreatic cancer and defined two distinct gemcitabine response-related phenotypes. Using machine learning algorithms, we constructed the MLDPP. Finally, we targeted a key signaling pathway, the C3a/C3aR pathway, whose activation promotes proliferation, migration and gemcitabine resistance in pancreatic cancer cells (Graphical abstract). The C3aR antagonist SB290157 effectively counteracted the above effects by inhibiting the activation of the C3a/C3aR pathway. These findings extend our current understanding of complement C3a and suggest that it is a promising biomarker and therapeutic target in pancreatic cancer.

Disclosure

NA.

Ethics statement

Approval of the research protocol by an Institutional Reviewer Board: The use of human samples was approved by the Ethics Committee of FUSCC with written informed consent from all patients and conducted according to the Declaration of Helsinki consent principles. Informed Consent: All informed consent was obtained from the subject(s) or guardian(s). Registry and the Registration No. of the study/trial: N/A. Animal Studies: All animal experiments were conducted in accordance with the Institutional Animal Care and Use Committee of FUSCC.

Funding information

This study was jointly supported by the National Natural Science Foundation of China (82303646, U21A20374 , 82173091, and 81701630), Shanghai Municipal Science and Technology Major Project (21JC1401500), Scientific Innovation Project of Shanghai Education Committee (2019-01-07-00-07-E00057), Clinical Research Plan of Shanghai Hospital Development Center (SHDC2020CR1006A), Xuhui District Artificial Intelligence Medical Hospital Cooperation Project (2021-011), Shanghai Natural Science Foundation (22ZR1412900), Research Project of Shanghai Municipal Health Commission (20214Y0396, 20194Y0375), and Shanghai Pujiang Program (21PJD014). The funding agencies had no role in study design, data collection, and analysis, decision to publish, or preparation of the manuscript.

Author contributions

SMS, LYY, and KZJ contributed equally to this work. SMS, LYY, and KZJ conceptualized and designed the experiment, and SMS wrote the first draft. SMS, LYY and KZJ conducted most of the molecular biology experiments and animal experiments, and analyzed the results. XJY, DCG and WDW critically revised drafts of the manuscript, provided important intellectual input, and approved the final version for publication. All authors read and approved the final manuscript.

CRediT authorship contribution statement

Duancheng Guo: Writing – review & editing, Methodology. **Weiding Wu:** Writing – review & editing, Supervision. **Xianjun Yu:** Supervision. **Longyun Ye:** Conceptualization. **Kaizhou Jin:** Supervision. **Saimeng Shi:** Writing – original draft, Conceptualization.

Declaration of Competing Interest

The authors declare that they have no known competing financial interests or personal relationships that could have appeared to influence the work reported in this paper.

Data availability

The data supporting the findings of this study are available within the article and its supplementary files. Source data are provided in this paper.

Appendix A. Supporting information

Supplementary data associated with this article can be found in the online version at doi:10.1016/j.csbj.2024.09.032.

References

[1] Siegel RL, et al. Cancer statistics, 2023. CA Cancer J Clin 2023;73(1):17–48.
[2] Mizrahi JD, et al. Pancreatic cancer. Lancet 2020;395(10242):2008–20.
[3] Stoffel EM, Brand RE, Goggins M. Pancreatic cancer: changing epidemiology and new approaches to risk assessment, early detection, and prevention. Gastroenterology 2023;164(5):752–65.
[4] Blackford AL, et al. Recent trends in the incidence and survival of stage 1A pancreatic cancer: a surveillance, epidemiology, and end results analysis. J Natl Cancer Inst 2020;112(11):1162–9.
[5] Binenbaum Y, Na'ara S, Gil Z. Gemcitabine resistance in pancreatic ductal adenocarcinoma. Drug Resist Updat 2015;23:55–68.
[6] Burris HA, et al. Improvements in survival and clinical benefit with gemcitabine as first-line therapy for patients with advanced pancreas cancer: a randomized trial. J Clin Oncol: J Am Soc Clin Oncol 1997;15(6):2403–13.
[7] Natu J, Nagaraju GP. Gemcitabine effects on tumor microenvironment of pancreatic ductal adenocarcinoma: Special focus on resistance mechanisms and metronomic therapies. Cancer Lett 2023;573:216382.
[8] Beutel AK, Halbrook CJ. Barriers and opportunities for gemcitabine in pancreatic cancer therapy. Am J Physiol Cell Physiol 2023;324(2):C540–52.
[9] Lin X, et al. Follicular helper T cells remodel the immune microenvironment of pancreatic cancer via secreting CXCL13 and IL-21. Cancers 2021;13(15).
[10] Bai X, et al. Adaptive antitumor immune response stimulated by bio-nanoparticle based vaccine and checkpoint blockade. J Exp Clin Cancer Res: CR 2022;41(1):132.
[11] Korbecki J, et al. CC Chemokines in a tumor: a review of pro-cancer and anti-cancer properties of receptors CCR5, CCR6, CCR7, CCR8, CCR9, and CCR10 Ligands. Int J Mol Sci 2020;21(20).
[12] Chen H, et al. Intratumoral delivery of CCL25 enhances immunotherapy against triple-negative breast cancer by recruiting CCR9+ T cells. Sci Adv 2020;6(5):eaax4690.
[13] Wu S, et al. CC chemokine ligand 21 enhances the immunogenicity of the breast cancer cell line MCF-7 upon assistance of TLR2. Carcinogenesis 2011;32(3):296–304.
[14] Correale P, et al. Tumor infiltration by T lymphocytes expressing chemokine receptor 7 (CCR7) is predictive of favorable outcome in patients with advanced colorectal carcinoma. Clin Cancer Res: J Am Assoc Cancer Res 2012;18(3):850–7.
[15] Wang S, et al. Blocking CD47 promotes antitumour immunity through CD103+ dendritic cell-NK cell axis in murine hepatocellular carcinoma model. J Hepatol 2022;77(2):467–78.
[16] Sanders KL, Fox BA, Bzik DJ. Attenuated toxoplasma gondii stimulates immunity to pancreatic cancer by manipulation of myeloid cell populations. Cancer Immunol Res 2015;3(8):891–901.
[17] Li Z, et al. The role of interleukin-18 in pancreatitis and pancreatic cancer. Cytokine Growth Factor Rev 2019;50:1–12.
[18] Wang ZW, et al. SRSF3-mediated regulation of N6-methyladenosine modification-related lncRNA ANRIL splicing promotes resistance of pancreatic cancer to gemcitabine. Cell Rep 2022;39(6):110813.
[19] Sabah A, et al. Enhancing web search result clustering model based on multiview multirepresentation consensus cluster ensemble (mmcc) approach. PloS One 2021;16(1):e0245264.
[20] Shi S, et al. Knockdown of TACC3 inhibits tumor cell proliferation and increases chemosensitivity in pancreatic cancer. Cell Death Dis 2023;14(11):778.
[21] Charoentong P, et al. Pan-cancer immunogenomic analyses reveal genotype-immunophenotype relationships and predictors of response to checkpoint blockade. Cell Rep 2017;18(1):248–62.
[22] Xu L, et al. TIP: a web server for resolving tumor immunophenotype profiling. Cancer Res 2018;78(23):6575–80.
[23] Chen B, et al. Profiling tumor infiltrating immune cells with CIBERSORT. Methods Mol Biol (Clifton, N J) 2018;1711:243–59.
[24] Jin Y, et al. Identification of novel subtypes based on ssGSEA in immune-related prognostic signature for tongue squamous cell carcinoma. Cancer Med 2021;10(23):8693–707.
[25] Aran D. Cell-type enrichment analysis of bulk transcriptomes using xCell. Methods Mol Biol (Clifton, N J) 2020;2120:263–76.
[26] Aran D, Hu Z, Butte AJ. xCell: digitally portraying the tissue cellular heterogeneity landscape. Genome Biol 2017;18(1):220.
[27] Li T, et al. TIMER: a web server for comprehensive analysis of tumor-infiltrating immune cells. Cancer Res 2017;77(21):e108–10.
[28] Li T, et al. TIMER2.0 for analysis of tumor-infiltrating immune cells. Nucleic Acids Res 2020;48(W1):W509–14.
[29] Finotello F, et al. Molecular and pharmacological modulators of the tumor immune contexture revealed by deconvolution of RNA-seq data. Genome Med 2019;11(1):34.
[30] Plattner C, Finotello F, Rieder D. Deconvoluting tumor-infiltrating immune cells from RNA-seq data using quanTIseq. Methods Enzymol 2020;636:261–85.
[31] Becht E, et al. Estimating the population abundance of tissue-infiltrating immune and stromal cell populations using gene expression. Genome Biol 2016;17(1):218.
[32] Racle J, et al. Simultaneous enumeration of cancer and immune cell types from bulk tumor gene expression data. ELife 2017;6.
[33] Zeng D, et al. Tumor microenvironment characterization in gastric cancer identifies prognostic and immunotherapeutically relevant gene signatures. Cancer Immunol Res 2019;7(5):737–50.
[34] Nishino M, et al. Revised RECIST guideline version 1.1: what oncologists want to know and what radiologists need to know. AJR. Am J Roentgenol 2010;195(2):281–9.
[35] Eisenhauer EA, et al. New response evaluation criteria in solid tumours: revised RECIST guideline (version 1.1). Eur J Cancer 2009;45(2):228–47.
[36] Perri G, et al. Radiographic and serologic predictors of pathologic major response to preoperative therapy for pancreatic cancer. Ann Surg 2021;273(4):806–13.
[37] Perri G, et al. Response and Survival associated with first-line FOLFIRINOX vs gemcitabine and nab-paclitaxel chemotherapy for localized pancreatic ductal adenocarcinoma. JAMA Surg 2020;155(9):832–9.
[38] Wishart DS, et al. DrugBank: a comprehensive resource for in silico drug discovery and exploration. Nucleic Acids Res 2006;34(Database issue):D668–72.
[39] Sherman MH, Beatty GL. Tumor microenvironment in pancreatic cancer pathogenesis and therapeutic resistance. Annu Rev Pathol 2023;18:123–48.
[40] Yin Z, et al. Macrophage-derived exosomal microRNA-501-3p promotes progression of pancreatic ductal adenocarcinoma through the TGFBR3-mediated TGF-β signaling pathway. J Exp Clin Cancer Res: CR 2019;38(1):310.
[41] Hou X, et al. HELLS, a chromatin remodeler is highly expressed in pancreatic cancer and downregulation of it impairs tumor growth and sensitizes to cisplatin by reexpressing the tumor suppressor TGFBR3. Cancer Med 2021;10(1):350–64.
[42] Liu J, Shi Y, Zhang Y. Multi-omics identification of an immunogenic cell death-related signature for clear cell renal cell carcinoma in the context of 3P medicine and based on a 101-combination machine learning computational framework. EPMA J 2023;14(2):275–305.

[43] Huan Q, et al. Machine learning-derived identification of prognostic signature for improving prognosis and drug response in patients with ovarian cancer. J Cell Mol Med 2023.
[44] Cancer Genome Atlas Research Network. Electronic address, a.a.d.h.e. and N. cancer genome atlas research, integrated genomic characterization of pancreatic ductal adenocarcinoma. Cancer Cell 2017;32(2):185–203. e13.
[45] Collisson EA, et al. Molecular subtypes of pancreatic cancer. Nat Rev Gastroenterol Hepatol 2019;16(4):207–20.
[46] Zarantonello A, et al. C3-dependent effector functions of complement. Immunol Rev 2023;313(1):120–38.
[47] Yadav MK, et al. Molecular basis of anaphylatoxin binding, activation, and signaling bias at complement receptors. Cell 2023;186(22):4956–73. e21.
[48] Gao S, Cui Z, Zhao MH. The complement C3a and C3a receptor pathway in kidney diseases. Front Immunol 2020;11:1875.
[49] Ajona D, Ortiz-Espinosa S, Pio R. Complement anaphylatoxins C3a and C5a: emerging roles in cancer progression and treatment. Semin Cell Dev Biol 2019;85:153–63.
[50] Zhang W, et al. Cntnap4 partial deficiency exacerbates alpha-synuclein pathology through astrocyte-microglia C3-C3aR pathway. Cell Death Dis 2023;14(4):285.
[51] Shu C, et al. C3a-C3aR signaling promotes breast cancer lung metastasis via modulating carcinoma associated fibroblasts. J Exp Clin Cancer Res: CR 2020;39(1):11.
[52] Gong B, et al. Complement C3a activates astrocytes to promote medulloblastoma progression through TNF-alpha. J Neuroinflamm 2022;19(1):159.
[53] Halbrook CJ, et al. Pancreatic cancer: advances and challenges. Cell 2023;186(8):1729–54.
[54] Afshar-Kharghan V. The role of the complement system in cancer. J Clin Invest 2017;127(3):780–9.
[55] Habermann JK, et al. Increased serum levels of complement C3a anaphylatoxin indicate the presence of colorectal tumors. Gastroenterology 2006;131(4).
[56] Cho MS, et al. Complement component 3 is regulated by TWIST1 and mediates epithelial-mesenchymal transition. J Immunol (Baltim, Md: 1950) 2016;196(3):1412–8.
[57] Aykut B, et al. The fungal mycobiome promotes pancreatic oncogenesis via activation of MBL. Nature 2019;574(7777):264–7.
[58] Suzuki R, et al. The complement C3a-C3a receptor axis regulates epithelial-to-mesenchymal transition by activating the ERK pathway in pancreatic ductal adenocarcinoma. Anticancer Res 2022;42(3):1207–15.
[59] Sodji QH, et al. The combination of radiotherapy and complement C3a inhibition potentiates natural killer cell functions against pancreatic cancer. Cancer Res Commun 2022;2(7):725–38.
[60] Hussain N, et al. Targeting the complement system in pancreatic cancer drug resistance: a novel therapeutic approach. Cancer Drug Resist 2022;5(2):317–27.
[61] Ajona D, Ortiz-Espinosa S, Pio R. Complement anaphylatoxins C3a and C5a: emerging roles in cancer progression and treatment. Semin Cell Dev Biol 2019;85:153–63.
[62] Zhu H, et al. Targeting the complement pathway in malignant glioma microenvironments. Front Cell Dev Biol 2021;9:657472.
[63] Grall M, et al. Eculizumab in gemcitabine-induced thrombotic microangiopathy: experience of the French thrombotic microangiopathies reference centre. BMC Nephrol 2021;22(1):267.
[64] MacDougall KN, et al. A case of gemcitabine-induced thrombotic microangiopathy treated with ravulizumab in a patient with stage IV pancreatic cancer. Cureus 2021;13(1):e13031.
[65] Brabletz S, et al. Dynamic EMT: a multi-tool for tumor progression. EMBO J 2021;40(18):e108647.
[66] Hussain N, et al. Targeting the complement system in pancreatic cancer drug resistance: a novel therapeutic approach. Cancer Drug Resist 2022;5(2):317–27.
[67] Zhang R, et al. Role of the complement system in the tumor microenvironment. Cancer Cell Int 2019;19:300.
[68] Markiewski MM, et al. Modulation of the antitumor immune response by complement. Nat Immunol 2008;9(11):1225–35.
[69] Ytting H, et al. Increased activity of the mannan-binding lectin complement activation pathway in patients with colorectal cancer. Scand J Gastroenterol 2004;39(7):674–9.